

Diverse Bases for Functional Spaces for Non-Rigid Shape Correspondence

Manika Bindal^{*}, Venkatesh Kamat^{*}

Discipline of Computer Science & Technology, Goa Business School, Goa University, Goa 403206, India

Corresponding Author Email: dcst.manika@unigoa.ac.in



Copyright: ©2024 The authors. This article is published by IETA and is licensed under the CC BY 4.0 license (<http://creativecommons.org/licenses/by/4.0/>).

<https://doi.org/10.18280/isi.290415>

ABSTRACT

Received: 31 March 2024

Revised: 23 July 2024

Accepted: 31 July 2024

Available online: 21 August 2024

Keywords:

non-rigid deformations, functional maps, basis functions, point-to-point correspondences

Computing meaningful correspondences for shapes undergoing non-rigid deformations is a fundamental task, challenging shape analysis community for many decades. The functional map framework has emerged as a powerful tool in this domain over the past decade due to its computational efficiency. Instead of tackling the combinatorial challenge of matching individual points across shapes, it focuses on constructing a linear mapping between the spaces of functions defined on these shapes. The map between function spaces is specified by a low-dimensional matrix obtained via suitably chosen basis functions that characterize the function space. This mapping can then be converted into a point-to-point correspondence between the shapes. The selection of an appropriate basis is a critical factor influencing the overall effectiveness and precision of the task. This survey explores various bases proposed to represent function spaces comprehensively within the realm of shape correspondence. Further insights into possible future directions are also provided.

1. INTRODUCTION

Advancements in 3D technology have made shape-based object recognition crucial, focusing on detailed geometric and topological information. These shapes exist independently of viewpoint, making shape analysis vital in computer vision, graphics, and geometry for understanding 3D shape properties and relationships that are essential for digital interaction. Shape analysis includes shape retrieval [1, 2], reconstructing the surface of shape from data points [3], meaningful segmentation [4], shape compression [5], and more.

Shape correspondence is a fundamental task that refers to matching two (or more) shapes in order to produce meaningful mapping between various elements of shapes [6]. Shape correspondence is crucial as the initial step in various applications like shape registration [7], symmetry detection [8], statistical shape modeling [9, 10], shape morphing [11], transfer of any attribute like deformation [12], texture [13], segmentation labels [14], transferring the style of one shape group to another [15]. These applications underscore its importance in effectively understanding, manipulating, and interacting with 3D shapes leading to enhanced object recognition and retrieval along with improved user experience in augmented and virtual reality applications. In Figure 1, a sparse point-to-point correspondence map between two cat shapes from the TOSCA Dataset [16] is depicted, highlighting the matching of corresponding body parts, say ears in both shapes. Although the research community has made significant progress in shape correspondence, further efforts are needed to develop techniques that effectively handle complex, noisy, and incomplete data, which will enhance the robustness and flexibility of real-world applications.

Shape matching methods are mainly designed and

categorized based on how shapes deform. Rigid deformation preserves Euclidean distances between points on a shape, while non-rigid deformation does not. Non-rigid deformations offer more flexibility in modeling shapes but also increase the complexity of shape correspondence problems [16]. To handle such variability, non-rigid deformations have traditionally been constrained to isometry, which restricts shape deformation by preserving surface distances between points. Bending a sheet of paper, folding a piece of cloth or twisting a pipe are few examples of isometric deformation. In Figure 2, the kid shape is shown in various poses, achieved by bending his legs and arms, illustrating isometric deformations. While rigid shape matching has been well addressed with efficient algorithms [17], non-rigid shape matching continues to be a major research focus due to the complex challenges posed by elastic, topological, and structural variations in shapes [18].

Based on the underlying representation of the shape, various methods have been proposed to compute shape correspondences. The geometry of a 3D shape can be represented via point cloud, surfaces, skeletons or volumes [19]. Surfaces can have implicit representation as level sets or can have an explicit representation as polygonal mesh, encapsulating both geometric as well as topological information [20]. For instance, the alignment of point clouds is achieved via RANSAC algorithm [21], surfaces are matched by identifying the underlying deformation [22], matching of shape skeletons is addressed in the work by Biasotti et al. [23], etc.

Shape correspondences can be computed directly through feature-based matching, iterative alignment with a few landmark points, or a hybrid approach that refines correspondences while searching for optimal alignment. Shape alignment involves finding a geometric transformation

to make shapes congruent and is primarily used for 3D object reconstruction [24] and, more recently, for reconstructing landscapes through time-varying registration [25]. Directly manipulating shape geometry is computationally demanding, necessitating alternative methods. Various approaches to compute shape correspondences are surveyed in [19, 26].

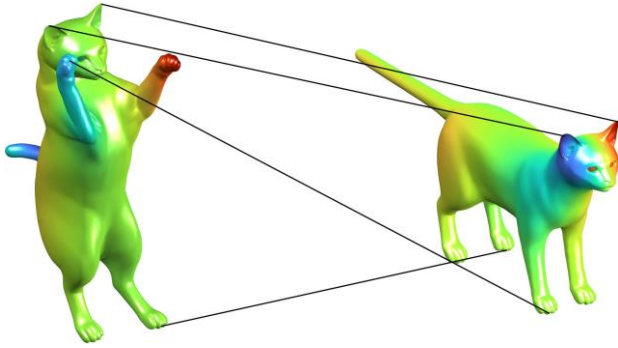


Figure 1. Meaningful point-to-point correspondences for sparse points for Cat shapes from TOSCA dataset [16]



Figure 2. Shapes from Kids Dataset subjected to isometric (or near-isometric) deformation depicting bending

Functional maps introduced by Ovsjanikov et al. [27] has addressed this challenge by transforming the problem of directly computing point-to-point correspondences to efficiently computing a linear mapping between functional spaces, defined on shapes. The computed linear functional map can then be utilized to recover point-to-point correspondences between shapes. Characterization of functional spaces is facilitated by the use of basis functions. By limiting the number of basis functions, shapes can be efficiently represented and processed in a lowdimensional space defined by the selected set of restricted basis functions.

The objective of this research work is to explore the following question within the context of functional maps for determining correspondences. How can different functional map bases be effectively used to represent and compute correspondences in non-rigidly deformed shapes, what properties and scenarios do they best address, and is there an optimal basis that provides a universal solution for various deformation complexities?

1.1 Related work

Functional maps, pioneered by Ovsjanikov et al. [27], revolutionized non-rigid shape correspondences. A SIGGRAPH Asia course [28] then distilled the essential

mathematical principles, incorporating the latest advancements. These maps showcase adaptability across vector field analysis [29], fluid simulation [30], mesh quadrangulation [31], and other shape analysis tasks. Despite their widespread use, selecting an ideal basis function remains a challenging area, crucial for accurate correspondence determination. Over time, researchers have proposed various basis functions, each with distinct strengths and weaknesses, elaborated in Section 5. Recently, Cammarasana and Patan'e [32] discusses various basis functions but restricts its examination to only Laplacian based basis functions utilized for various shape analysis tasks.

1.2 Scope

This survey paper comprehensively addresses the diverse range of basis functions proposed and employed particularly for non-rigid shape correspondence till date. The underlying principles, limitations and practical implications involved in utilizing different basis functions is thoroughly discussed. Basis functions are analysed based on the properties they exhibit across parameters like orthogonality, compactness (i.e., the ability of a few basis functions to effectively capture necessary details for shape matching), consistency in handling isometric or non-isometric deformations across diverse shapes, the capacity to capture global aspects of shape or offer local support, and robustness against topological noise. These aspects and more are discussed in detail in Section 6. This paper seeks to serve as a comprehensive reference point for researchers, students, academicians and practitioners in shape matching, who want to stay updated on the latest advancements in this field, guiding them to the optimal basis functions for their specific needs.

1.3 Organization

The survey paper is organized as follows. Section 2 formally introduces the problem of shape correspondence along with its diverse classifications. Various underlying representations of shapes are also provided. Section 3 discusses multiple approaches suggested to solve the correspondence problem. Section 4 delves into the mathematical foundations of functional maps, incorporating latest developments. Section 5 thoroughly provides a detailed historical account of basis functions and presents their desired characteristics. Section 6 provides the comparative analysis of basis functions highlighting in tabular form the properties fulfilled by each basis. Section 7 provides possible future directions for functional map bases with respect to non-rigid shape correspondence. Section 8 summarizes the work.

1.4 Notations

Following notations are used in this paper. S and X are continuous and discrete representations of the surface of a shape respectively. η is point-to-point map between shapes, while η_F is the functional representation of η . Continuous version of Laplace-Beltrami Operator is specified as Δ_X .

W_X represents cotangent-weight matrix and D_X is a lumped mass matrix for shape X . ICP means Iterative Closest Point. LBO means Laplace-Beltrami Operator. CQHB stands for Coupled-quasi Harmonic basis. CMM is Compressed Manifold Modes. LMH means Localized Manifold Harmonics. HO is Hamiltonian Operator. CMH means Coordinate

Manifold Harmonics. LAB is Landmark Adapted Basis functions.

1.5 Datasets

This study employs TOSCA Dataset [16], KIDS Dataset [33], SHREC 2010 [34] and SHREC 2019 Datasets [35].

2. OVERVIEW

2.1 Shapes

Kendall [36] described a shape as *all the geometrical information that remains when location, scale, and rotational effects are filtered out from an object*. However, this definition only considers Euclidean distances and doesn't handle shapes undergoing non-rigid deformations. In computer graphics, various techniques, such as Constructive Solid Geometry (CSG), Voxel Representation, and Boundary Representation (B-rep), etc. are employed to describe shapes. Among these, B-rep is preferred due to its superior flexibility and efficiency in compactly representing shapes [37]. In geometry processing, shapes are characterized as the 2D surfaces defining the boundaries of tangible 3D objects. Varied shape representations are categorized into the continuous and discrete as follows:

2.1.1 Continuous shape representations

Surface of a shape can be defined as an orientable continuous 2D-manifold embedded in \mathbb{R}^3 [20]. Mathematically, continuous surfaces (S) can be specified either by a parametric representation or by an implicit representation. Parametric surfaces are vector function $f: \Omega \rightarrow S$ mapping a parameter domain $\Omega \in \mathbb{R}^2$ onto a surface $S \in \mathbb{R}^3$. Spline and subdivision surfaces [38] are examples of parametric representations of shape. Implicit (or volumetric) representation is the zero set of a scalar-valued function $S: \mathbb{R}^3 \rightarrow \mathbb{R}$ i.e. $S = \{x \in \mathbb{R}^3 \mid S(x) = 0\}$. Signed-distance fields [39] and level sets [40] describe implicit representations of surfaces. For complex shapes, a single function approximating the entire surface is impractical. Instead, a piecewise approach is used, approximating the surface locally with global tolerances. Triangles or quadrangles are used for parametric surfaces, while hexahedral (voxels) or tetrahedral cells represent implicit surfaces in a piecewise manner.

2.1.2 Discrete shape representations

Surface of a shape can be defined as an orientable continuous 2D-manifold. For computation, a polygon mesh and point cloud are the discrete representations of a shape (see Figure 3). A 2D polygon mesh $M = (V, E, F)$ embedded in 3D is a collection of vertices V , edges E and faces F , approximating the smooth surface with a piece-wise linear mapping containing both geometric and topological information of the shape. Each vertex $v_i \in V$ is a 3D coordinate (x_i, y_i, z_i) in ambient space. Mesh faces are usually convex polygons of various shapes (triangles, quadrilaterals, etc.) with shared edges limited to two faces per edge. Triangular meshes are preferred due to hardware optimization and efficiency. A polyhedral mesh is similar but includes volumetric cells. Point clouds represent shapes with only vertices in \mathbb{R}^3 , lacking connectivity information [41]. Levoy and Whitted [42] proposed to use point clouds for enhanced

efficiency in displaying landscape scenes due to increasing visual complexity.

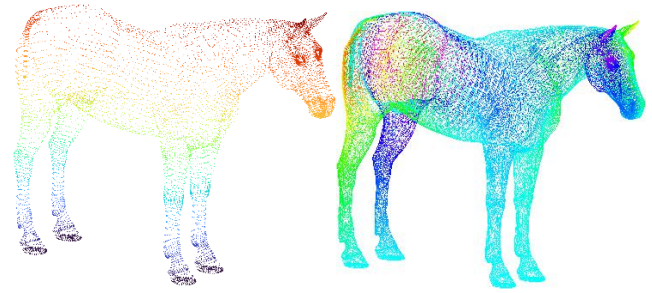


Figure 3. Geometry of horse shape represented as point cloud (left) and a triangular mesh (right) from TOSCA Dataset [16]

2.2 Shape correspondence

Shape correspondence problem can be formally stated as: Given n shapes $S_1, S_2, S_3, \dots, S_n$ find a meaningful relation (or mapping) R among the elements (points, skeletal attributes, or components) of these shapes. Two elements $a \in S_1$ and $b \in S_2$ are said to be in correspondence if $(a, b) \in R$. Meaningful map entails understanding the shape structure and functionality both at the global and the local level. The map can be constrained as one-to-one, one-to-many or many-to-many depending upon the application [19]. A point-to-point map between two discrete shapes X_1 and X_2 is expressed as $\eta: X_1 \rightarrow X_2$ such that $\forall x_1 \in X_1 \mid \exists \eta(x_1) \in X_2$. If both the shapes contain same number of points, then η is a bijection. Computing this mapping involves accurately connecting specific points, like ensuring the left ear of one cat shape corresponds precisely to the left ear of another (see Figure 1). However, identifying matching points between shapes leads to an exponential increase in possible solutions, with complexity $O(n!)$, making the problem NP-hard. Various aspects of correspondence problems have been explored as follows:

Full vs Partial Matching Depending on the presence of missing or additional components in shapes relative to each other, correspondence mapping may involve matching all elements (full match) or selectively matching certain elements, indicating a partial match. Partial shape matching presents additional challenges as seen in Figure 4 with shapes such as an animal horse and a mythological creature centaur from the TOSCA dataset [16]. Despite global dissimilarities between shapes, certain components, like their bottom parts, may match, significantly increasing the search space [43].

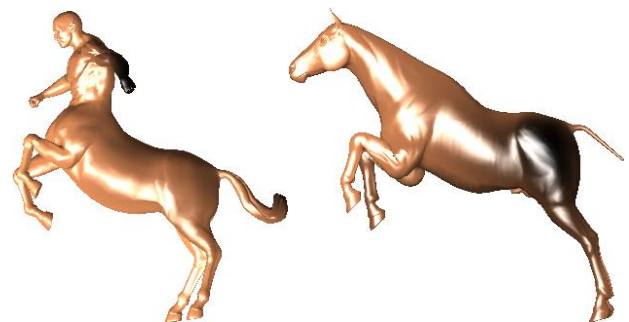


Figure 4. Partial shape matching between a Horse and a Centaur from TOSCA dataset [16], where bottom parts of both shapes match

Sparse vs Dense Correspondences Based on the density of correspondences, all (dense) or few (sparse) of the elements are matched. Matching key components like hands, legs, head of cat shapes as depicted in Figure 1 offers valuable insights into cat shape semantics [44]. However, applications like shape morphing and attribute transfer demand dense correspondences for achieving global smoothness [45]. Directly computing a dense correspondence map is infeasible, so various methods resort to obtaining sparse correspondences first and then extend them to dense correspondences [46].

2.2.1 Rigid shape matching

When a shape undergoes transformation such that the pairwise euclidean distances remain unchanged, determining correspondences for such shapes, have traditionally been posed as a rigid alignment (or registration) problem. Under the assumption of rigidity, a shape can be deformed via geometric transformations like rotation, translation and reflection or their compositions. Rigid registration seeks to obtain an optimal rigid transformation that aligns two shapes. Iterative Closest Point (ICP) [47] is a renowned method for establishing pointwise correspondences between shapes. This local-search algorithm iteratively determines correspondences while minimizing distances between corresponding points, often using a variant of Hausdorff distance [48]. However, ICP's performance is significantly influenced by its initial alignment, which is a consequence of its greedy optimization. To address occlusions and topological noise, efficient versions of ICP [49] have been developed. Recently, Zhang et al. [50] introduced a faster and more robust version of ICP, boasting improved convergence rates.

2.2.2 Non-rigid shape matching

While rigid shape matching techniques have seen success, their effectiveness is constrained in practical situations due to the diverse poses and deformations shapes can undergo. Variations in pairwise Euclidean distances are significant, as seen in Figure 5, where shapes can experience complex non-rigid deformations such as stretching around shoulders (Figure 5a) and topological changes induced by self-contact (Figure 5b), making it difficult to establish meaningful pointwise correspondences. To facilitate mathematical analysis of shapes experiencing non-rigid deformations and expedite correspondence searching, the traditional approach mainly restricts deformations to isometry or approximate-isometry, as depicted in Figure 2. Isometric deformations aim to maintain geodesic distances [51, 52] between points on a shape's surface, a property common in real-world organic shapes. Elad and Kimmel [6] employed pose-invariant embeddings using intrinsic geodesic distances for correspondence determination. Bronstein et al. [53] utilized a joint similarity criterion, balancing intrinsic and extrinsic measures, to improve pointwise correspondences. Introducing stretching into deformations escalates the complexity of non-rigid shape matching. For instance, matching an elephant with a gorilla presents a more challenging non-isometric shape matching problem than matching two elephants in different poses. Addressing this complexity, Kim et al. [54] introduced a fully automatic technique to compute a low-distortion and smooth correspondence map between non-isometrically deformed shapes. Yet, this method doesn't readily apply to partial shape matching, as it computes a global mapping without considering localization aspects. For a comprehensive exploration of non-rigid shape correspondences, readers are

urged to consult the insights provided in the study of Bronstein et al. [16].

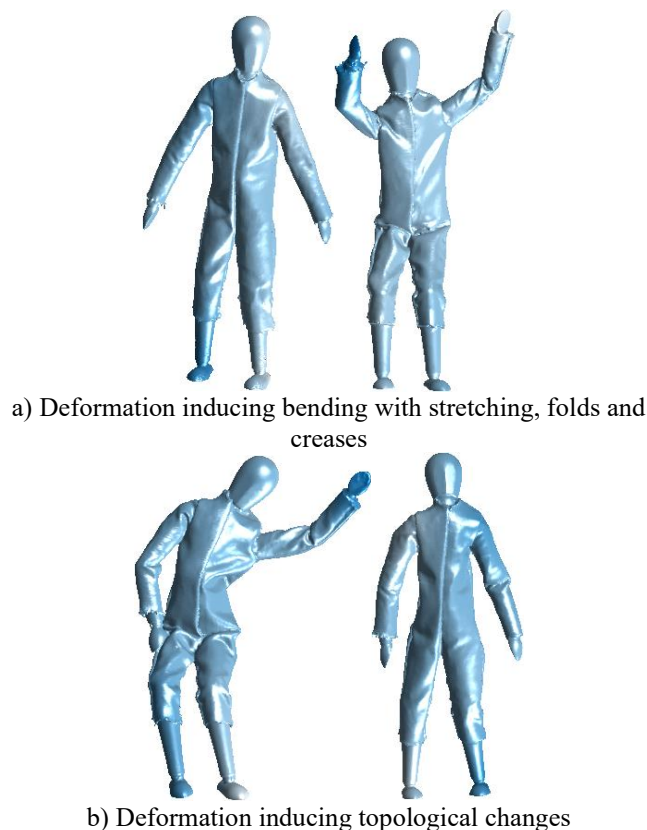


Figure 5. Shapes of articulated wooden mannequins from SHREC 2019 Dataset [35] subjected to various non-rigid deformations

3. SHAPE CORRESPONDENCE APPROACHES

Shape correspondence, a longstanding challenge, has driven various techniques in the shape analysis community. Correspondence maps can be estimated through registration, alignment-based, similarity-based, or learning-based approaches, as outlined below:

3.1 Registration or alignment based approaches

Registration-based approaches align shapes by deforming the source shape to the target or aligning both shapes to a common domain through parametrization [25]. Once aligned, pointwise correspondence is established by identifying proximal points. This alignment is achieved by seeking a geometric transformation that aligns the shapes. Chang and Zwicker [55] aim for piece-wise rigid alignment by applying transformations to localized segments of the shape, rather than seeking a global transformation (refer Section 2.2.1). To register shapes undergoing non-rigid deformations, a regularization is introduced to ensure similarity of transformations across spatially proximate points, effectively determining a deformation field for the source shape. Deng et al. [25] investigated non-rigid registration schemes based solely on geometric information, while Saiti and Theoharis [56] explored the registration of multimodal shape data with differing underlying structures, dimensions, densities, and noise levels.

3.2 Similarity based approaches

Computing correspondences directly involves deriving geometric invariants and feature descriptors for different shape elements, tailored to the specific type of deformation. These descriptors include pointwise surface descriptors such as GPS [57], HKS [58, 59], and WKS [60], or pairwise descriptors like geodesic distances [51], biharmonic distances [61], etc., used for shapes undergoing isometric deformations.

Recent techniques have championed the use of learning-based descriptors including parametric spectral descriptors [62], descriptors learnt considering no known deformation model between the shapes [63], robust descriptors with relatively less training data learnt from raw shapes [64]. These descriptors form an objective function that maximizes descriptor similarity while minimizing potential deformation without explicit alignment [65]. The objective function is optimized using well-known continuous optimization techniques, such as linear programming in the study by Berg et al. [66], convex optimization in the study by Zass and Shashua [67], or discrete optimization techniques as utilized in the study by Zhang et al. [45] via tree-based searches.

3.2.1 Embeddings

By embedding shapes in a lower-dimensional geometric feature space, a hybrid method simplifies the registration process. Correspondences are then inferred from spatial relationships within this common space. The embeddings can be determined either as isometric or spectral embedding. Isometric embedding refers to a mapping or transformation of geometric objects in such a way that the pairwise distances on the surface of shape remain unchanged [6]. However, by leveraging the spectral properties of mesh operators, spectral methods offer robust and efficient means to access inherent geometric structure of shapes [68]. These techniques that are used for directly computing pointwise correspondences give rise to challenging non-linear optimization problems that lack convexity, posing significant challenges in terms of solution. Introducing global constraints into such problems also inherently complicates the optimization process.

3.2.2 Functional maps

The mathematical idea of functional maps was introduced in the study [27] to match near-isometric manifolds. It aims at obtaining a linear map between spaces of functions defined on the shapes, by matching feature descriptors posed as real-valued functions. Functional map determines the similarity of real-valued functions defined on shapes and can be compactly represented as a low-rank matrix given a choice of basis functions. Once the functional map is computed, it is converted efficiently to obtain point-to-point correspondences between shapes. It is an automatic method and does not depend on the user input in the form of priors and is computationally quite efficient as it, in a sense, linearise the challenging non-rigid shape correspondence problem. Since the introduction of functional maps in the geometry processing community, it has become a key building block for varied shape analysis tasks. Refer Section 4 for an in-depth discussion of functional maps.

3.3 Learning based approaches

Methods based on machine learning and deep neural networks are also demonstrating promising capabilities concerning shape correspondence [69]. Xu et al. [70] proposed

various data-driven techniques for determining correspondences. For robust generalization, supervised methods need large datasets, while unsupervised alternatives, though class-agnostic and annotation-free, may lag in performance compared to supervised counterparts [71]. Learning-based methods still suffer from over-fitting, heavy dependence on application-specific shape priors and data augmentation apart from being computationally expensive, limiting their use in resource-constrained settings [64]. Recently Abdelreheem et al. [72] exploited capabilities of large language and vision models to determine non-isometric shape matching.

4. FUNCTIONAL MAPS

Ovsjanikov et al. [27] introduced a coordinate free, independent of underlying geometric representation of shapes, computationally efficient functional map framework that utilizes the idea of functional maps to compute point-to-point correspondences between shapes. Instead of directly comparing physical coordinates of shapes, functional maps operate in a higher-level space of geometric functions. Formally, on a shape \mathcal{S} , a real-valued function is specified as $f: \mathcal{S} \rightarrow \mathbb{R}$ describing some geometric property like curvature or surface distance from a specific point to all other points on the shape, etc. (refer Figure 6). Consider $F(\mathcal{S}, \mathbb{R})$ as the generic space of such scalar-valued functions defined on the shape \mathcal{S} . For two shapes \mathcal{S}_1 and \mathcal{S}_2 equipped with functional spaces $F(\mathcal{S}_1, \mathbb{R})$ and $F(\mathcal{S}_2, \mathbb{R})$ respectively, a point-to-point bijective correspondence map is specified as $\eta: \mathcal{S}_1 \rightarrow \mathcal{S}_2$, which induces a natural transformation $\eta_F: F(\mathcal{S}_1, \mathbb{R}) \rightarrow F(\mathcal{S}_2, \mathbb{R})$, a unique functional map between two function spaces, also known as the functional representation of map η . Hence, for any function $f_1 \in F(\mathcal{S}_1, \mathbb{R})$, a corresponding function $f_2 \in F(\mathcal{S}_2, \mathbb{R})$ can be obtained via functional map as $f_2 = \eta_F(f_1)$ or derived via composition as $f_2 = f_1 \circ \eta^{-1}$. Note that, however complex η may be, η_F operates linearly between function spaces and the knowledge of η_F is equivalent to knowledge of η . Refer to the study by Ovsjanikov et al. [27] for proofs.



Figure 6. Real-valued functions visualized on wolf shape from TOSCA dataset [16] depicting geodesic distances from different source points (left; right) and mean curvature (middle) (colours from blue to red indicate small to high values)

Let the space $F(\mathcal{S}_1, \mathbb{R})$ be characterized by a basis $\{\phi_i\}_{i \geq 1}$ such that any function $f_1 \in F(\mathcal{S}_1, \mathbb{R})$ can be expressed as linear combination of basis functions as $f_1 = \sum_i \alpha_i \phi_i$, where α_i are representation coefficients that can be identified by projecting the function f_1 on each basis function ϕ_i . Since η_F is a linear mapping, $\eta_F(f_1) = \eta_F(\sum_i \alpha_i \phi_i) = \sum_i \alpha_i \eta_F(\phi_i)$. Simultaneously, if the function space $F(\mathcal{S}_2, \mathbb{R})$ is characterized by basis $\{\psi_j\}_{j \geq 1}$, then $\eta_F(\phi_i) = \sum_j \beta_{ji} \psi_j$ for some $\{\beta_{ji}\}$ such that:

$$\eta_F(f_1) = \sum_j \sum_i \alpha_i \beta_{ji} \psi_j \quad (1)$$

If f_1 is represented as a coefficient vector $\mathbf{a} = (\alpha_0, \alpha_1, \dots, \alpha_i, \dots)$ and $f_2 = \eta_F(f_1)$ as a vector $\mathbf{b} = (b_0, b_1, \dots, b_i, \dots)$, then Eq. (1) signifies $b_j = \sum_i \beta_{ji} \alpha_i$ where β_{ji} is the j^{th} coefficient of i^{th} basis function of $F(S_1, \mathbb{R})$ which has been mapped to $F(S_2, \mathbb{R})$ i.e. j^{th} coefficient of $\eta_F(\phi_i)$ expressed in basis ψ_j . Note that β_{ji} is solely determined by the basis and the map η , and is independent of f_1 . If basis functions $\{\psi_i\}$ are orthonormal with respect to some inner product $\langle \cdot, \cdot \rangle$ as $\beta_{ji} = \langle \eta_F(\phi_i), \psi_j \rangle$ then $\{\beta_{ji}\}$ denoted by \mathbf{C} has a simple structure. Consider shapes \mathcal{X}_1 and \mathcal{X}_2 as the discrete representation of shapes, sampled at n points with basis matrices $\Phi, \Psi \in \mathbb{R}^{n \times k}$ comprising of only k basis functions for both shapes respectively, then a linear functional map η_F can be expressed via a matrix $\mathbf{C} \in \mathbb{R}^{k \times k}$ that intuitively maps coefficients from one shape's basis to the other. For any function $f_1 \in F(\mathcal{X}_1, \mathbb{R})$, represented as a coefficient vector \mathbf{a} , the functional map acts on the vector as $\eta_F(\mathbf{a}) = \mathbf{C}\mathbf{a}$ fully encoding the underlying pointwise correspondence map η .

4.1 Determining functional map

Identification of a correspondence map between shapes amounts to determining functional map η_F and then convert it into point-to-point correspondences (refer Section 4.2). Functional map framework consists of various steps. First step is to determine feature descriptors on each shape that are essentially real-valued functions and are expected to remain invariant under the desired mapping. Examples of such descriptor functions are mentioned in Section 3.2. Once the descriptor functions have been identified for both the shapes, next step is to determine basis for the respective function spaces such that descriptor functions can be efficiently represented and utilized as constraints for computing η_F . Laplace-beltrami operator (LBO) eigenfunctions are utilized as basis functions in the original work of functional maps [27] which are essentially Fourier basis on manifolds [73, 74]. LBO eigenfunctions are a preferred choice for basis as only few eigenfunctions are required to represent most natural functions on shape and due to the stability of the space of functions spanned by these eigenbasis under deformations. Please refer Section 5 for more details on the properties a basis function should possess. Next step is to estimate the functional map \mathbf{C} by solving the following optimization problem in the least squares sense:

$$\mathbf{C}_{\text{opt}} = \arg \min_{\mathbf{C}} E_{\text{desc}}(\mathbf{C}) + \mu E_{\text{reg}}(\mathbf{C}) \quad (2)$$

where first term preserves the descriptor functions, μ is a scalar weight parameter and the second term regularizes the map by emphasizing the accuracy of its overall structural characteristics. Orthogonality of the functional map ensures the presence of an underlying point-to-point map; hence Eq. (2) is solved such that $\mathbf{C}^T \mathbf{C} = \mathbf{I}$. Note that \mathbf{C} , the resulting functional map is unaffected by the number of shape points, making it efficient, especially for high-resolution shapes. Functional maps, due to its compactness, computational efficiency, and the capacity to seamlessly transfer information across different shapes, have emerged as a powerful technique to match non-rigid shapes.

4.2 From functional maps to correspondences

Once functional map η_F has been optimized as discussed in

Section 4.1, the underlying point-to-point map η which induces η_F is desired. Consider Φ and Ψ as k -dimensional point clouds and obtained functional map \mathbf{C} being orthogonal, can be considered a rigid alignment transformation between them. Set $\mathbf{C}_0 = \mathbf{C}$. For every i^{th} row of $\Psi \mathbf{C}_0^T$, find the closest row j_i in Φ via nearest-neighbour algorithm. Solve for an optimal and orthonormal \mathbf{C} minimising $\sum_i \|\Phi_{j_i} - \Psi \mathbf{C}^T\|_2$ and set $\mathbf{C}_0 = \mathbf{C}$. These operations are repeated convergence. In short, establishing point-to-point correspondences from a functional map relies on the rigid ICP alignment of spectral coordinates Φ and Ψ in k -dimensional spectral domain.

4.3 Improvements in functional maps

Over time, a multitude of alternative regularization techniques and extensions have been suggested, leading to substantial enhancements in the accuracy of estimation of functional maps and hence point-to-point correspondences. Determination of functional map has been improved by dealing with unknown ordering of descriptor functional constraints [44], by adding a geometric structure on the functional map matrix and considering both rows and columns as functions on respective shapes [75], by proposing to consider descriptor functions as linear operators ensuring improved underlying pointwise map [76], by proposing a regularizer consisting of a bounded Laplacian operator ensuring structural preservation of functional maps [77]. ZoomOut [78], a promising end-to-end technique that progressively expands the size of functional basis, while alternating between optimization of functional map and computation of point-to-point mapping. By exhibiting a particular structure on the functional map, Rodolà et al. [79] extended maps to deal with partial shape matching. In order to enhance the resilience of functional maps to diverse mesh tessellations and to refine the precision of pointwise correspondences, a technique involving map deblurring and denoising was introduced by Ezuz and Ben-Chen [80]. While continuous optimization techniques like ADMM and MADMM have dominated the field of optimal basis and functional map optimization for the past decade, Ren et al. [81] introduced a promising discrete solver designed specifically for energies based on functional maps.

5. BASIS FOR FUNCTIONAL MAPS

Basis functions are essential in the functional map framework, defining the space for shape computation. Initially used for space classification and theorem proving, they have evolved to analyze spaces across domains. Following reasons also establishes the significance of basis functions in the functional mapping of shapes:

Efficiency Functional maps represented via small number of basis functions results in significantly improved computational efficiency and reduced storage requirements particularly for high-resolution shapes.

Robustness Basis functions are resilient against noise and deformations, leading to heavy utilization for real-world shape analysis tasks.

The choice of appropriate basis functions is crucial for improving the precision of point-to-point correspondences achieved through the functional map approach. Section 5.1 discusses various desirable properties that a basis should exhibit in order to describe the space of functions defined on

shapes.

5.1 Desirable properties of basis functions

Basis functions should incorporate characteristics that capture critical geometric aspects of the shape. Following are preferred properties that a basis should possess:

(1) **Completeness:** All linear combinations of basis functions should be able to represent the entire space of functions defined on shape, regardless of the complexity of its geometry.

(2) **Compactness:** Basis should be compact i.e. most natural shape functions should be spanned by a compact basis, a property crucial for efficient storage and processing of shapes.

(3) **Stability:** The basis functions should be chosen such that the space spanned by their linear combinations remains unaffected by shape deformations.

(4) **Orthogonality:** By ensuring independence of each basis function via orthogonality, it simplifies the representation and manipulation of shapes.

(5) **Multi-Scale Property:** Basis functions should be able to effectively capture features at different scales within the shape. Large-scale features representing global aspects of shape geometry while small-scale features depicting finer details.

(6) **Smoothness:** Smooth basis functions provide continuous representation of shapes by reducing artifacts and providing a more visually pleasing representation.

(7) **Computational Efficiency:** Basis should be easy to compute and evaluate as this property becomes crucial while processing large number of shapes together.

(8) **Numerical Stability:** Numerical stability is desired so as to prevent divergence and instability in the algorithms that use them.

(9) **Consistency:** Basis should be consistent when computed across multiple shapes i.e. they should be seamlessly compatible and robust under minor violations of deformation invariance.

(10) **Locality:** Basis functions should encode behaviour of functions in the neighbourhood of a given point. Locally-supported basis functions capture shape deformations which is essential aspect of effective shape correspondence.

In addition to the aforementioned properties, it is advantageous for the basis functions to exhibit robustness to topological changes. The choice of a basis for shape representation will depend on the specific application and the trade-offs between these properties.

5.2 Proposed basis functions

In order to compute functional mapping between two shapes, various basis functions have been proposed since the utilization of functional maps in shape analysis community, specifically for computing point-to-point correspondences. A comprehensive overview of all such basis is provided as follows:

5.2.1 Laplace-beltrami operator eigenfunctions

For a shape \mathcal{S} and a scalar field $f: \mathcal{S} \rightarrow \mathbb{R}$, the self-adjoint Laplace-Beltrami operator (LBO) $\Delta_{\mathcal{S}}$ describing intrinsic aspects of shape is defined as the negative divergence of the gradient of scalar field as $\Delta_{\mathcal{S}} f = -\text{div}(\nabla f)$ and subsequently admits an eigendecomposition with non-negative eigenvalues λ and corresponding orthonormal eigenfunctions

ϕ , via $\Delta_{\mathcal{S}} \phi = \lambda \phi$. The eigenfunctions of LBO (refer Figure 7a) also known as *manifold harmonics* [82] characterizes geometric and topological properties of shapes and has been utilized to parametrize the linear functional map in the study by Ovsjanikov et al. [27] as basis function, owing to its compactness, stability, orthogonality, isometric invariance and multi-scale capability. The LBO eigenbasis is in principle similar to Fourier basis defined on a Euclidean domain.

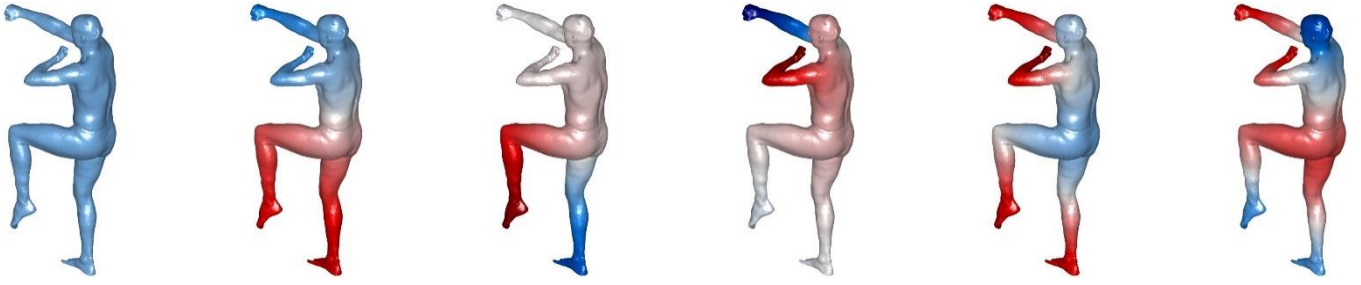
Laplace-Beltrami operator $\Delta_{\mathcal{S}}$ is independent of any global coordinate system and of the underlying representation of shape i.e. meshes, point clouds, volumes, etc. For the operator, varied consistent discretizations have been proposed [83, 84] in the literature. Popularly, for triangle meshes, LBO can be effectively discretized using the cotangent scheme, yielding a representation expressed as $L = D^{-1}W$ captures local geometry of the shape and is computed based on angles between edges, and D is a lumped mass matrix containing consolidated information about vertex areas [85]. Recently, Bunge and Botsch [86] comprehensively investigated the discrete LBO for general polygon meshes. While Belkin et al. [87] explored LBO for point clouds. The eigendecomposition of discrete LBO is a generalized eigenvalue problem $W\Phi = D\Phi\Lambda$ which can be numerically posed as the minimization problem:

$$\underset{\Phi}{\text{argmin}} \text{tr}(\Phi^T W \Phi) \quad \text{st} \quad \Phi^T D \Phi = I \quad (3)$$

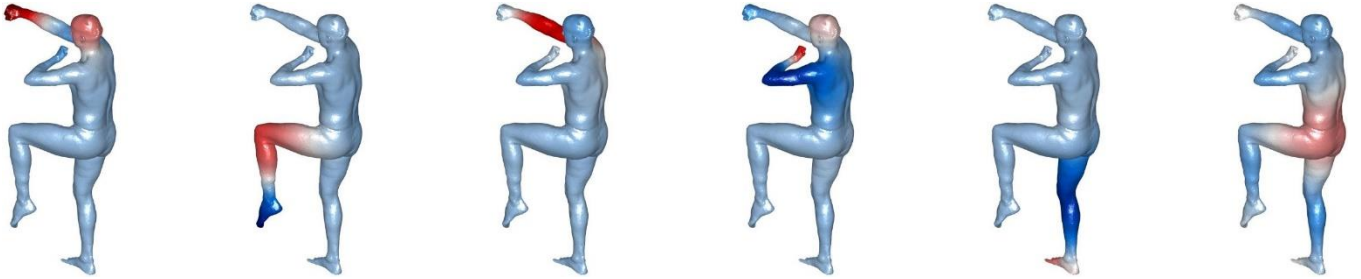
To represent smooth functions on shape with bounded variation, LBO eigenbasis have been proved to be optimal [88] being complete, compact, orthogonal, multi-scale and computationally quite efficient. Despite being constructed in a local manner, LBO eigenbasis contain global information of the shape and is considered as the workhorse of geometry processing especially for isometrically deformed shapes. However, even for slight deviations in the isometric deformations, low-frequency basis possess no theoretical guarantees for having consistent behaviour across shapes. LBO eigenbasis capture global aspect of shapes, are robust to local topological changes and are sensitive to local geometric details resulting in numerical instability for basis functions representing higher frequencies [86]. Learning-based methods also acknowledge the challenges posed by LBO eigenbasis and seek improved basis for shape correspondence [89], despite its heavy utilization.

5.2.2 Coupled-quasi harmonic basis

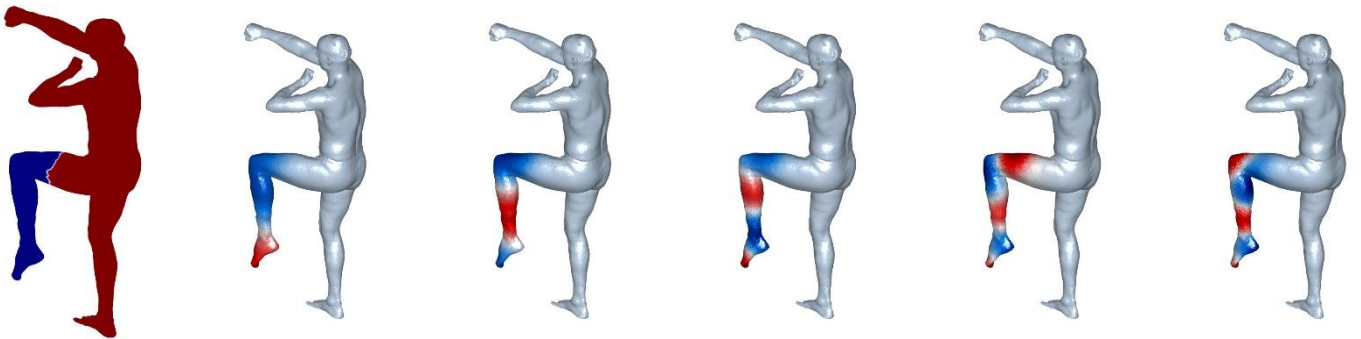
Computing the correspondence between shapes, wherein the deformation is not only restricted to isometry but also include stretching and beyond, consistency among shape basis becomes a crucial property. The idea of coupled-quasi harmonic basis (CQHB) was subsequently introduced in the study by Kovnatsky et al. [90] to accommodate shapes with stretching along with matching non-isometric shapes, for example, a human shape can be semantically matched with that of a gorilla. For two shapes represented as triangle meshes \mathcal{X}_1 and \mathcal{X}_2 , coupled bases Φ and Ψ are desired, which approximately diagonalizes their respective Laplace-Beltrami Operators. Each basis function is desired to be coupled as $\{\Phi\}_i \approx \{\Psi\}_i \circ \eta^{-1}$ and can be obtained by solving the approximate joint diagonalization problem specified as non-linear optimization with orthogonality constraints:



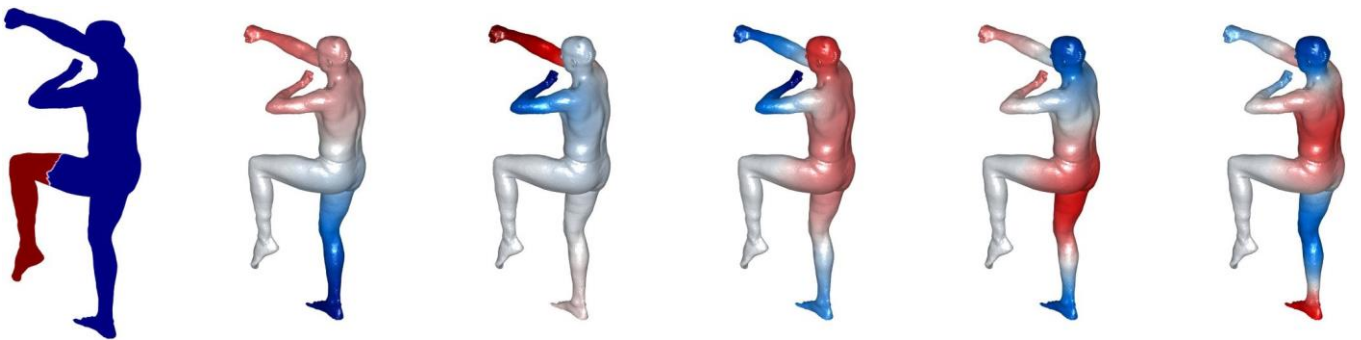
a) Eigenfunctions of the Laplace-Beltrami Operator without local support, characterizing the shape on a global scale



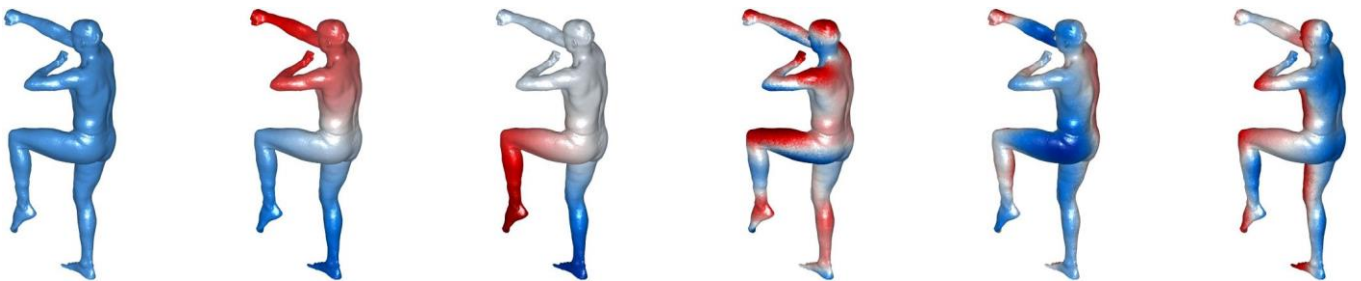
b) Compressed Manifold Modes offering localized support and capturing meaningful structural components of the shape



c) Manifold Harmonics localized within the explicitly defined region (in blue) corresponding to the left leg of a human shape



d) Eigenfunctions of the Hamiltonian operator featuring a step potential function, with the leftmost shape displaying color-coded regions (red denoting high-potential areas and blue indicating low-potential regions)



e) Coordinate Manifold Harmonics, with the first three figures illustrating intrinsic information via standard LBO eigenfunctions and the subsequent three figures representing extrinsic information through the coordinates x , y and z

Figure 7. Examining the localization characteristics of different basis functions, illustrated on human shape from SHREC 2010 dataset [34] through visual comparisons

$$\begin{aligned} & \text{off}(\Phi^T W_{x_1} \Phi) + \text{off}(\Psi^T W_{x_2} \Psi) + \\ \underset{\Phi, \Psi}{\text{argmin}} & \quad \left\| F_{x_1}^T \Phi - F_{x_2}^T \Psi \right\|_F^2 \quad (4) \\ \text{st} & \quad \Phi^T D_{x_1} \Phi = I, \quad \Psi^T D_{x_2} \Psi = I \end{aligned}$$

where ‘‘off’’ denotes the summation of the squares of all off-diagonal elements, $W_{\mathcal{X}}$ represents cotangent weight matrix and $D_{\mathcal{X}}$ is a lumped mass matrix for shape \mathcal{X} . The descriptor functions for respective shapes are represented as $F_{\mathcal{X}}$ that are preserved under isometric deformations and are utilized as constraint for coupling the basis. Though it handles non-isometric nature of shape deformations better compared to LBO basis, the theoretical framework for CQHB is still actively expanding to make it computationally more efficient.

5.2.3 Compressed manifold modes

The global spatial support of LBO eigenbasis poses a significant challenge while interpreting them as descriptors for specific regions of the shape and in addition sensitivity to topological noise is higher, in the presence of holes and occlusions. Compressed Manifold Modes (CMM) [91] overcomes this issue by enhancing LBO eigenbasis for triangle mesh \mathcal{X} with local support. The sparsity-inducing l_1 -regularization lets the shape be processed as a collection of parts by solving the following optimization problem:

$$\underset{\Phi}{\text{argmin}} \text{tr}(\Phi^T W \Phi) + \mu \|\Phi\|_1 \quad \text{st} \quad \Phi^T D_{x_1} \Phi = I \quad (5)$$

where μ is the parameter to handle local support of the basis (larger μ means smaller support region), W and D are as specified in Section 5.2.1 and is solved by utilizing an iterative scheme Alternating Direction Method of Multipliers (ADMM) algorithm [92]. Manifold Alternating Directions Method of Multipliers (MADMM), proposed by Kovnatsky et al. [93] is an efficient way to compute CMMs which optimizes the basis on Stiefel manifold of orthogonal matrices [94]. CMMs (refer Figure 7b) are invariant to isometric deformations, orthogonal, robust to geometric and topological noise and performs better than LBO eigenbasis especially while dealing with partial shape matching. Haas et al. [95] streamlined CMM eigenfunction calculation for optimal shape coverage. However, CMMs still exhibit computational inefficiency and lack a multi-scale nature required for hierarchical processing of shapes.

5.2.4 Localized manifold harmonics

While CMM does offer local support, it lacks explicit control over localization and doesn't guarantee a global solution. Melzi et al. [96] proposed *Localized Manifold Harmonics* (LMH) where localization can be controlled in an explicit and computationally efficient manner by specifying a region of interest on the surface. LMH expands the LBO eigenbasis for triangular mesh \mathcal{X} through an incremental construction process, wherein new basis functions are ensured to be orthogonal to the existing set of basis functions. It is obtained by spectrally decomposing a modified LBO through the solution of the generalized eigenvalue problem represented as $Q \Psi = D \Psi \Lambda$. The following numerical formulation is provided to yield eigenfunctions with localized support as:

$$\underset{\Psi}{\text{argmin}} \text{tr}(\Psi^T Q \Psi) \quad \text{st} \quad \Psi^T D \Psi = I \quad (6)$$

where $Q = W + \mu_R D \text{diag}(v) + \mu_{\perp} D \Phi \Phi^T D$ is the modified

Laplacian operator. The modified operator is also symmetric, positive semi-definite and intrinsic along with its eigenfunctions. Section 5.2.1 defines W and D as usual cotangent weight and area matrices respectively. $\mu_R > 0$ is a support region parameter while $\mu_{\perp} > 0$ specify parameter for orthogonality of LMH with respect to precomputed LBO basis Φ , v is the discrete version of membership function for the region defined explicitly. LMH are isometry-invariant, smooth and captures sharp details from specified region along with retaining the global structure. With respect to point-to-point correspondences, LMH enhances capability of existing LBO eigenbasis to beautifully incorporate local information in a compact manner. Nevertheless, there persists a challenge in pinpointing regions within the shape (refer Figure 7c) that must be explicitly supplied to modified operator (Q) for the purpose of improving correspondences, such as the identification of areas exhibiting high reconstruction error.

5.2.5 Hamiltonian operator basis

The LBO eigenbasis is globally sensitive to shape topology, hindering accurate matching, especially for complex shapes where detailed localized features are crucial. Originating from quantum mechanics, the Hamiltonian operator (HO), well-known for its role in Schrödinger's equation, was adapted for shape analysis in the study of Choukroun et al. [97] to represent sharp features using its eigenfunctions. This is achieved by modifying manifold harmonics so that its localization properties can be utilized and be computationally viable for spectral analysis. On the shape \mathcal{S} , given a scalar potential function $v: \mathcal{S} \rightarrow \mathbb{R}_+$, Hamiltonian Operator $\mathcal{H}_{\mathcal{S}}$ is the generalization of Laplace-Beltrami operator $\Delta_{\mathcal{S}}$ operating on $f \in \mathcal{S}$ as $\mathcal{H}_{\mathcal{S}}(f) = \Delta_{\mathcal{S}}(f) + \mu v(f)$ with parameter $\mu \in \mathbb{R}$. In the discrete setting, for triangle mesh \mathcal{X} , Hamiltonian Operator can be specified via LBO's cotangent weight matrix W and D respectively and the potential function v is applied diagonally. Self-adjointness is preserved under addition of Hamiltonian operators, enabling eigendecomposition through a generalized eigenvalue problem $(W + \mu D \text{diag}(v)) \Phi = D \Phi \Lambda$ which can numerically be posed as the respective optimization as:

$$\underset{\Phi}{\text{argmin}} \text{tr}(\Phi^T W \Phi) + \mu \text{tr}(\Phi^T \text{diag}(v) \Phi) \quad (7) \\ \text{st} \quad \Phi^T D \Phi = I$$

with parameter μ balancing global and local support of the Hamiltonian eigenbasis. The Hamiltonian's distinctive feature is its ability to concentrate harmonics within arbitrary manifold subsets using step potential functions across the domain (refer Figure 7d). Rampini et al. [98] utilized alignment of Hamiltonian Operator's eigenvalues for partial shape matching without actually solving for underlying pointwise correspondences. Hamiltonian eigenbasis with compact support are more noise-robust. Postolache et al. [99] provided a theoretical analysis and a unifying approach to using Hamiltonian eigenfunctions with the functional map framework, achieving state-of-the-art results in partial shape matching.

5.2.6 Coordinate manifold harmonics

The dimensionality of the basis function, traditionally determined empirically, indicates the number of required functions to preserve and recover a shape's geometric details efficiently. By adding three supplementary functions to standard manifold harmonics, Coordinate Manifold

Harmonics (CMH) [100] significantly enhance the preservation of local isometries. This enhancement results in a more robust representation of shape geometry, effectively capturing both intrinsic and extrinsic information from the shapes (refer Figure 7e). To standard LBO eigenfunctions (Φ) computed for shape \mathcal{X} represented as a polygonal mesh, a set of three basis functions ϕ_x, ϕ_y, ϕ_z are added. These basis functions contain extrinsic information, which is captured by orthogonal projection of representation error of the low-pass filter representation of $x, y,$ and z -coordinates of all the vertices of the shape respectively. The representation error is $\Sigma = \Phi\Phi^T DX - X$ with x -coordinate of shape \mathcal{X} specified as X with the basis function given as $\phi_x = \Sigma - (\Phi\Phi^T D \Sigma)$ which can be normalized further. Similar to ϕ_x , other basis functions ϕ_y and ϕ_z can be computed by replacing X with low-pass filter representation of y and z coordinates respectively. CMH, designed for tessellation transfer and incorporating extrinsic information, requires shapes in similar poses due to its reliance on vertex coordinates [101].

5.2.7 Data-driven basis

While the LBO emphasizes low-frequency eigenfunctions to enhance smoothness, Azencot and Lai [102] introduced an adaptive basis that facilitates improved feature matching. By integrating the computation of functional maps with the design of basis functions, authors have been able to create a cohesive and unified framework for determining correspondences. Considering two shapes \mathcal{X}_1 and \mathcal{X}_2 represented as triangle meshes, with corresponding descriptor functions F_1 and F_2 , the objective is to calculate the basis B_1 and B_2 for each shape while concurrently establishing a functional map \mathbf{C} . This functional map aims to optimally align the descriptor functions for both shapes as:

$$\min_{B_1, B_2, C} \frac{1}{2} |C B_1^T F_1 - B_2^T F_2|_{\mathcal{F}} \quad \text{st } B_1^T D_1 B_1 = I, B_2^T D_2 B_2 = I \quad (8)$$

This optimization problem exhibits complex non-linearity, non-convexity, and involves a high degree of dimensionality. To decrease dimensionality, the authors suggested employing Proper Orthogonal Decomposition (POD) modes offering improved spectral representation for high-frequency signals. These modes expand the solution space by employing feature descriptors with multiple degrees of freedom. By integrating regularization terms that encourage smoothness, consistency and isometry, the optimization process is carried out using the Alternating Direction Method of Multipliers (ADMM). While data-driven bases favor descriptor similarity on shapes, high-frequency-tuned bases show less uniform correspondence. Accuracy in shape correspondence is sensitive to subspace choice and size. Larger subspaces improve scalar function representation but require extra regularization to avoid local minima and undesired solutions. These bases adapt to the input shapes. Similar to the concept of deriving insights directly from data, Marin et al. [103] suggested that basis learned through machine learning techniques exhibit resilience and contribute to enhanced accuracy in demanding scenarios. Though it also ends up learning descriptor features along with the basis, it does not exploit the underlying geometric structure of the shape.

5.2.8 Landmark adapted basis

In texture transfer, artists pinpoint landmark

correspondences that must be preserved and expanded into a detailed, time-efficient, and adaptable point-to-point map for non-isometric deformations. While landmark correspondences are used as descriptor preservation constraints in the functional map framework to resolve symmetry ambiguities, they are not always precisely preserved in the dense map.

Panine et al. [104] introduced orthogonal landmark adapted basis functions (LAB), combining solutions of Dirichlet-Steklov and Dirichlet-Laplacian eigenproblems. These functions precisely preserve landmark correspondences and promote conformal maps between shapes. For a shape \mathcal{X} represented as triangle mesh, discrete Dirichlet-Laplacian eigenproblem is specified via cotangent LBO as $W\Phi = D\Phi$ such that $\Phi|_{\partial\mathcal{X}} = 0$. For the same shape \mathcal{X} , consider that the boundary $\partial\mathcal{X}$ consists of two disjoint non-empty open sets denoted by D and P , then discrete Dirichlet-Steklov eigenvalue problem is specified as: $W\Psi = P\Psi$ such that $\Psi|_D = 0$ where the non-lumped Steklov mass matrix is given by:

$$\mathcal{P}_{pq} = \begin{cases} \frac{1}{3}(r_{p-1} + r_{p+1}) & , p = q \text{ and } p, q \in \partial\mathcal{X} \\ \frac{1}{6}r_{pq} & , p \sim q \text{ and } p, q \in \partial\mathcal{X} \\ 0 & , \text{elsewhere} \end{cases}$$

where the length of edge connecting vertices p and q is r_{pq} . The computed correspondences exhibit improved accuracy for non-isometric shapes. Overall, the suggested approach is descriptor-free, demonstrating efficiency and robustness in handling substantial variations in mesh structures. Note that LAB functions are capable of handling meshes with significant topological variations in connectivity and in noise.

5.2.9 Elastic basis

Computing correspondences for shapes that undergo non-isometric deformations, especially when the goal is to align extrinsic features, presents a considerable challenge. In addressing this challenge, Hartwig et al. [105] introduced a crease-aware elastic basis that is non-orthogonal. This basis is derived from the Hessian of elastic thin shell energy, capturing bending and stretching properties influenced by shell thickness. For reduced thickness, the bending energy significantly impacts eigenmodes characterized by smaller eigenvalues, making these modes more susceptible to curvature features. The eigenmodes of the Hessian, arranged by ascending eigenvalues, symbolize deformations organized according to their associated elastic energy. The elastic basis, unlike previously proposed bases used in functional maps, is not orthogonal, posing challenges for standard functional map computations. Hence, the authors have also modified the functional map framework to effectively compute point-to-point correspondences with these non-orthogonal basis. We refer the reader to Algorithm (1) in the study [105] to gain insight into the precise methodology for computing point-to-point correspondences via elastic basis for triangular mesh. The elastic basis requires that the triangle meshes under consideration should be regular in order to achieve desired results.

5.3 Other operators and basis

While the shape analysis community has extensively studied operators both within and outside the functional framework, their ability to establish correspondences between

non-rigid shapes has been largely overlooked. This thorough examination of basis functions explores the potential of these unexplored operators within functional maps, encouraging further research and analysis.

Extrinsic Operators Addressing the complexities of non-rigid shapes, especially their susceptibility to transformations and prevalence in natural settings, non-rigid shape correspondence research has prioritized intrinsic aspects as reliable features. However, Liu et al. [106] counter this notion, highlighting limitations in intrinsic measurements' ability to discern surface protrusion directionality. To capture extrinsic aspects of the shapes in an explicit manner, Liu et al. [106] introduced a family of Dirac operators $L(\tau) = (1 - \tau)\Delta_{\mathcal{X}} + \tau D_N$, which by varying $\tau \in [0,1]$ captures the entire spectrum of intrinsic and extrinsic features from shape \mathcal{X} depending upon the desired task. Note $\Delta_{\mathcal{X}}$ is Laplace-Beltrami Operator is purely intrinsic in nature and D_N refers to relative Dirac operator which is purely extrinsic in nature and is based on the Gauss map. To this end, Andreux et al. [107] proposed Anisotropic LBO, which incorporates variability in principal curvature directions, capturing both intrinsic and extrinsic shape aspects. Wang et al. [108] introduced the Steklov operator, encoding volumetric geometry by treating the 2D surface as the boundary of its 3D interior. This operator is robust to topological changes and offers strong localization capabilities. While the Dirac operator efficiently captures surface features, the Steklov operator excels in capturing volumetric information.

Indicator Basis The LBO eigenbasis effectively captures smooth functions and low-frequency components but struggles with high-frequency details and non-smooth functions like step functions. Melzi [109] introduced the Indicator basis to improve this, showing promise for transferring region indicator functions between shapes via functional maps. However, careful vertex sampling is essential for complete representation of the indicator function basis across the surface.

Shell Operator Shapes containing topological noise, possessing intrinsic self-similarities and deviating from isometric deformations require robust basis functions to improve pointwise shape correspondences under such challenging scenarios. Corman et al. [110] proposed a functional shape difference-based approach to encode both intrinsic and extrinsic shape properties. Eisenberger et al. [111] integrated intrinsic and extrinsic aspects by embedding shapes in a product space of LBO basis (intrinsic) and Cartesian coordinates with outer normals (extrinsic). They use smooth shells as coarse-to-fine shape approximations, aligning them iteratively with minimal geometric changes to establish functional maps and point-to-point correspondences between shapes.

6. COMPARATIVE ANALYSIS OF BASES

Methodology: Multiple ordered basis functions for a single shape have been computed using MATLAB. The first six basis functions are visualized on the shape with colours ranging from red to blue. As shown in Figure 7, this visualization helps understand the properties captured by each basis. Following are the observations.

Observations: Popularly utilized Laplace-Beltrami Operator eigenbasis, which are natural harmonic basis functions defined on the shape is a preferred choice mainly due to its well-

established theoretical foundations along with multi-scale capability, orthogonality and invariance to isometric deformations. However, when shape deformations deviate from isometric to non-isometric, consistency of LBO eigenbasis become questionable as they are computed independently for each shape. LBO basis especially while representing high-frequencies are numerically unstable. Coupled-quasi harmonic basis (CQHB) introduced the idea to jointly diagonalize the LBO for the shapes under consideration so as to retain consistency among such deviations in deformations but are computationally expensive over LBO basis. Regardless of less robust theoretical grounding in comparison to LBO, CQHB shines in its joint construction for multiple shapes. This facilitates compatibility, direct comparison, and ultimately, more accurate non-rigid shape correspondences.

LBO eigenfunctions characterizes the global information of shape but by construction is not capable of localization. Hence, LBO eigenbasis complicates shape interpretation in parts, hindering partial shape matching and subsequently requires infinite (or very high) number of basis functions to represent sharper details of shapes. Compressed Manifold modes (CMMs) and Localised Manifold harmonics (LMH) address this issue by providing local support allowing shapes to be interpreted as a collection of parts. CMMs localised via l_1 -sparsity regularization are orthogonal, local, smooth and robust to topological noise present in shapes, but are computationally quite intensive. LMH are computationally as efficient as LBO eigenbasis and retains theoretical guarantees and are flexible in regulating and providing local support which makes them quite impressive for many practical applications like for semantically-guided interventions. LMH performs better in capturing sharp details with a few localized harmonics compared to large number of LBO basis when aiming to represent the same level of detail in a given region and also to mitigate influence of topological noise. While LMH effectively addresses various desirable characteristics for isometric shape matching, the need to provide valuable information like the region of support and precomputed LBO basis in order to derive newly computed basis in an orthogonal manner introduces an additional complexity. The inclusion of these extra tasks have contributed to relatively limited popularity of LMH in comparison to other basis. Various attempts have been made to introduce localization in basis functions, so that better and meaningful details can be captured via functional map framework (refer Figure 7). The introduction of step potential in Hamiltonian Operator serves as a form of guided localization over the vibrational modes occurring on the surface and a lack of underlying global structure makes Hamiltonian basis an organic choice for partial shape matching.

Unlike LBO eigenbasis, Coordinate Manifold Harmonics (CMH) incorporates extrinsic information by utilizing spatial coordinates of the shapes. This capability proves invaluable in shape matching scenarios, especially when dealing with shapes that share intrinsic similarities but vary in their overall spatial positioning. For example, a cardboard sheet and a cylinder crafted from that same sheet are similar from intrinsic aspect but differs while considering extrinsic features.

While CQHB and data-driven basis may seem analogous in their approach by taking shapes as input and determining the basis in a coupled manner, a crucial distinction arises. CQHB operates on the assumption that a smooth function space is encompassed by its basis, aiming to diagonalize the LBO and

thus favouring smooth basis functions. In contrast, this is not applicable to data-driven basis, which does not inherently prioritize the smoothness of the basis functions. Unlike methods developed for matching isometrically deformed shapes, the elastic basis aligns creases and folds accurately and robustly, leading to more accurate correspondences for non-isometric shapes. Its various characteristics, including non-orthogonality, feature sensitivity, and multi-scale representation is preferred over conventional orthogonal basis.

Landmark Adapted Basis, by exactly preserving the provided landmark correspondences as desired by certain texture transfer applications in a time-efficient manner, is unlike any other proposed basis functions. LAB while preserving landmarks, also caters to non-isometrically deformed shapes. Indicator basis excels at transferring step functions i.e. highly non-smooth functions between shapes which is an uphill task for other discussed smooth operator basis.

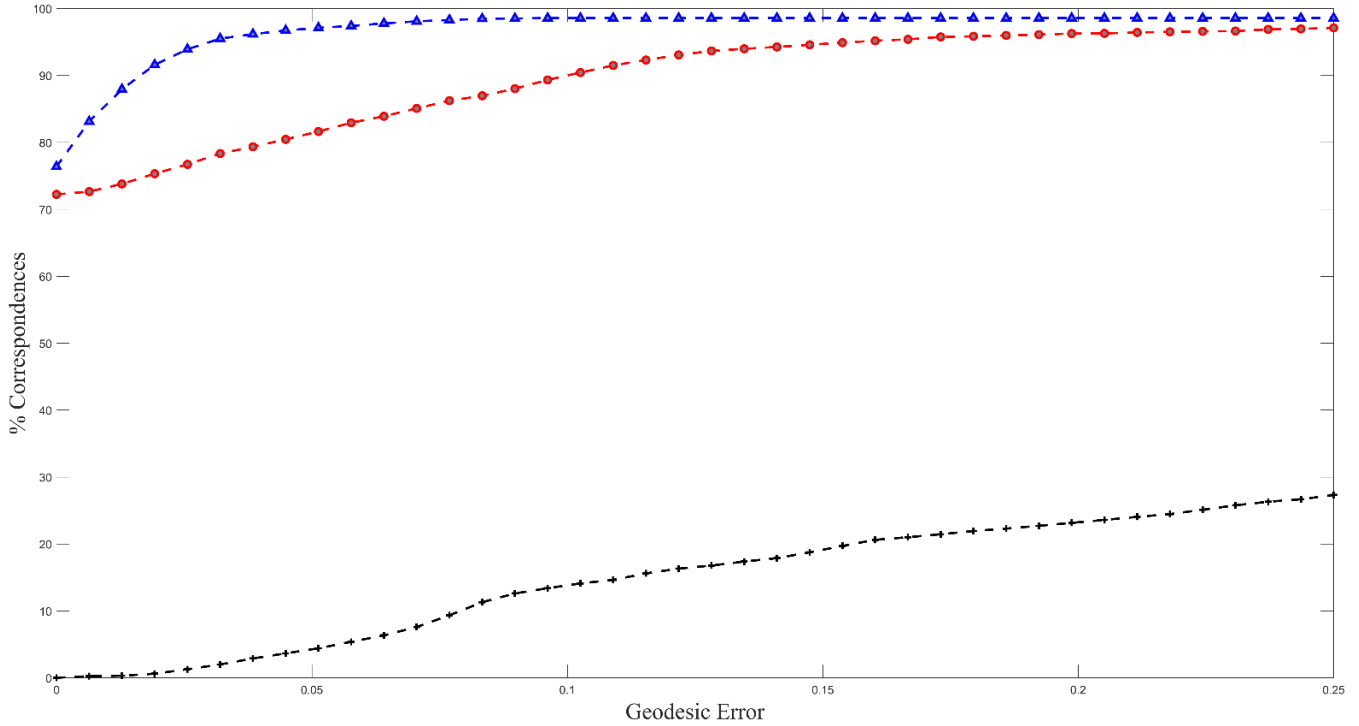


Figure 8. Point-to-point correspondence accuracy for the wolf mesh using different bases within the functional framework: Laplace-Beltrami eigenfunctions (blue line with triangle markers), Hamiltonian eigenfunctions (red line with circular markers), and compressed manifold modes (black line with plus markers)

Table 1. Diverse Basis Functions employed in Non-rigid Shape Correspondence, satisfying distinct properties

| | LBO Basis [82] | CMM [91] | CQHB [90] | LMH [96] | CMH [100] | HO Basis [97] | Data-Driven Basis [102] | Elastic Basis [105] | LAB [104] |
|--|----------------|----------|-----------|----------|-----------|---------------|-------------------------|---------------------|-----------|
| Completeness | ✓ | ✓ | | ✓ | ✓ | ✓ | | | ✓ |
| Compactness | ✓ | | | ✓ | ✓ | ✓ | | ✓ | ✓ |
| Stability | ✓ | ✓ | ✓ | ✓ | ✓ | ✓ | | | ✓ |
| Orthogonality | ✓ | ✓ | ✓ | ✓ | ✓ | ✓ | ✗ | ✗ | ✓* |
| Multi-scale Property | ✓ | ✗ | ✓ | ✓ | ✓ | ✓ | ✗ | ✓ | ✓ |
| Smoothness | ✓ | ✓ | ✓ | ✓ | ✓ | ✓ | ✓* | ✓ | ✓ |
| Computational Efficiency | ✓ | ✗ | ✗ | ✓ | ✓ | ✓ | ✓* | ✗ | ✓* |
| Numerical Stability | ✓* | ✓ | ✓ | ✓ | ✓ | ✓ | ✓* | ✓* | ✓* |
| Consistency for Isometric deformations | ✓ | ✓ | ✓ | ✓ | ✓ | ✓ | ✓* | ✗ | ✗ |
| Consistency for Non-Isometric deformations | ✗ | ✗ | ✓ | ✗ | ✗ | ✗ | ✓* | ✓ | ✓ |
| Local Support | ✗ | ✓ | ✗ | ✓ | ✗ | ✓* | ✓* | ✗ | ✓* |
| Global Support | ✓ | ✗ | ✓ | ✓ | ✓ | ✓* | ✓ | ✓ | ✓* |
| Robustness to Topological Noise | ✗ | ✓ | ✓ | ✓ | ✗ | ✓ | ✓ | ✗ | ✓ |
| Shared-bases | ✗ | ✗ | ✓ | ✗ | ✗ | ✗ | ✓ | ✗ | ✗ |

(✓ specifies property is completely satisfied, ✓* means property is satisfied given certain conditions, ✗ means property is not satisfied, "" (space) means property has not been studied for respective basis in literature so far). For a rapid reference, consult the notations provided in Section 1.4

Table 1 provides a summary of various functional basis used for non-rigid shape correspondence, indicating their adherence to specific properties. Symbols such as \checkmark denote property is completely satisfied, \checkmark^* signifies that the property is satisfied under certain conditions, \times indicates non-satisfaction of the property, and a " " (space) implies that the property has not been studied for the respective basis in the existing literature.

In order to visually compare the localization aspects exhibited by various basis functions see Figure 7. LBO eigenfunctions with no local support is shown in Figure 7a; CMMs as shown in Figure 7b captures meaningful local regions of human shape like hands, legs, head, etc., making it effective to use for partial shape matching. CMH as shown in Figure 7e captures intrinsic (three leftmost shapes) as well as extrinsic information based on spatial coordinates (three rightmost shapes). LMH shown in Figure 7c with leftmost shape depicting the region in blue explicitly provided to restrict the information captured in that region. By incorporating the step potential function such that red region indicating high-potential region and blue region indicating low-potential region is shown in leftmost shape of Figure 7d. Hamiltonian operator basis functions capture details from low potential region while avoiding high-potential region in Figure 7d.

Consider wolf shapes in two different poses from TOSCA dataset [16] for which point-to-point correspondences are computed via functional maps keeping all variables constant except the basis functions. This enables analysis of how basis function changes impact correspondence map accuracy. Refer to Figure 8 for the accuracy of point-to-point correspondences, expressed as the percentage of correct matches relative to the total number of vertices on the shapes, calculated using the LBO basis, Hamiltonian basis, and CMMs.

7. DISCUSSION AND FUTURE SCOPE

Based on existing literature of computing point-to-point correspondences for non-rigid shapes via functional maps, several promising research directions are provided as follows:

- Despite demonstrating powerful capability of Laplace-Beltrami operator eigenfunctions in the case of near-isometric shapes, the task of determining basis for functional spaces of partial and non-isometric shapes, remains a challenging area.
- Irrespective of the varied basis functions proposed to obtain enhanced non-rigid shape correspondences, it still remains the major challenge as to theoretically determine how many basis functions are sufficient for the task and the given resolution of shapes.
- Various operators as discussed in Section 5.3 have not yet been explored in the context of functional maps, as to how the eigenfunctions of such operators behave when considered as basis functions.
- For Hamiltonian Operator, so far only step potential function has been explored in the context of partial shape matching. Other smoother potential functions can be investigated further to see if they improve pointwise correspondences between shapes [98].
- Functional maps, initially designed for orthogonality and now extended to accommodate non-orthogonal Elastic basis has opened up new avenues for exploring basis functions beyond traditional constraints [105].
- Despite beautiful descriptors proposed to capture details from shape, identifying a descriptor function that is able to

capture both local and global geometry of the surface and is simultaneously stable with respect to both isometric and non-isometric deformations is still an open problem [100].

- The Landmark Adapted Basis exhibits dense clustering of Dirichlet-Steklov eigenfunctions around landmarks, indicating the potential for alternative basis with more dispersed functions to enhance behaviour near these landmark points [104].

- Bases functions discussed in Section 5.2 have been designed with a primary focus on shapes represented as triangle meshes, excluding the widely known LBO. Exploring additional shape representations, as outlined in Section 2.1, presents opportunities for further investigation with respect to basis functions.

To summarize, the findings show that future research in non-rigid shape correspondences via functional maps includes exploring bases for partial and non-isometric shapes, determining the optimal number of basis functions, and investigating eigenfunctions from various operators. For the Hamiltonian Operator, examining smoother potential functions may improve correspondences. Extending functional maps to nonorthogonal Elastic bases and developing descriptor functions that capture both local and global geometries while being stable for all deformations are key challenges. Additionally, refining Landmark Adapted Basis and exploring basis functions for different shape representations, like triangle meshes, could enhance accuracy.

8. CONCLUSIONS

This survey explores various basis functions proposed in the functional map framework within the context of non-rigid shape correspondence in a comprehensive manner. Different functional map bases can be effectively used to represent and compute correspondences in non-rigidly deformed shapes by leveraging their unique properties tailored to specific deformation scenarios. The Laplace-Beltrami Operator (LBO) eigenbasis is ideal for isometric deformations due to its strong theoretical foundation and multi-scale capabilities, while the Coupled-Quasi Harmonic Basis (CQHB) addresses non-isometric deformations with improved consistency but higher computational costs. Localized bases like Compressed Manifold Modes (CMMs) and Localized Manifold Harmonics (LMH) provide local support for capturing detailed features and handling partial shape matching. Hamiltonian Operator Eigenfunctions are suited for partial matching due to their guided localization, and Coordinate Manifold Harmonics (CMH) incorporate extrinsic information, useful for shapes with spatial variations. Elastic Basis excels in aligning creases and folds in non-isometric shapes, and Landmark Adapted Basis (LAB) precisely preserves landmark correspondences.

Overall, no single basis offers a universal solution for all deformation complexities. Trade-offs exist between theoretical rigour, computational efficiency, and desired properties like local support and multi-scale analysis. Orthogonality and smoothness of basis, which has been synonymous with functional maps since its inception have now taken a back seat, with localization and incorporating extrinsic features in non-rigid shape analysis as emerging focus. Integrating consistency, handling varied tessellations, dealing with non-isometric real-world data, preserving attributes as demanded by artists and still being able to automatize the process of shape matching are the kind of

themes, around which basis functions are being looked at. Though various learning-based approaches are coming up to determine functional maps, they tend to be oblivious to the underlying geometry of the shape and moreover in resource-constrained settings fixed basis functions are preferred.

ACKNOWLEDGMENT

This work was financially supported by the Visvesvaraya PhD Scheme, funded by the Ministry of Electronics and Information Technology, Government of India (Grant No.: VISPHD-MEITY-1090).

REFERENCES

- [1] Tangelder, J.W., Velkamp, R.C. (2008). A survey of content based 3D shape retrieval methods. *Multimedia Tools and Applications*, 39(3): 441-471. <https://doi.org/10.1007/s11042-007-0181-0>
- [2] Gasparetto, A., Minello, G., Torsello, A. (2015). Non-parametric spectral model for shape retrieval. In *Proceedings of the 2015 International Conference on 3D Vision*, Lyon, France, pp. 344-352. <https://doi.org/10.1109/3DV.2015.46>
- [3] Berger, M., Levine, J.A., Nonato, L.G., Taubin, G., Silva, C.T. (2013). A benchmark for surface reconstruction. *ACM Transactions on Graphics*, 32(2): 1-17. <https://doi.org/10.1145/2451236.2451246>
- [4] Shamir, A. (2008). A survey on mesh segmentation techniques. *Computer Graphics Forum*, 27(6): 1539-1556. <https://doi.org/10.1111/j.1467-8659.2007.01103.x>
- [5] Maglo, G., Lavoué, G., Dupont, F., Hudelot, C. (2015). 3D mesh compression: Survey, comparisons, and emerging trends. *ACM Computing Surveys*, 47(3): 1-41. <https://doi.org/10.1145/2693443>
- [6] Elad, D., Kimmel, R. (2003). On bending invariant signatures for surfaces. *IEEE Transactions on Pattern Analysis and Machine Intelligence*, 25(10): 1285-1295. <https://doi.org/10.1109/TPAMI.2003.1233902>
- [7] Tam, G.K., Cheng, Z.Q., Lai, Y.K., Langbein, F.C., Liu, Y., Marshall, D., Martin, R.R., Sun, X.F., Rosin, P.L. (2013). Registration of 3D point clouds and meshes: A survey from rigid to nonrigid. *IEEE Transactions on Visualization and Computer Graphics*, 19(7): 1199-1217. <https://doi.org/10.1109/TVCG.2012.310>
- [8] Mitra, N.J., Pauly, M., Wand, M., Ceylan, D. (2013). Symmetry in 3D geometry: Extraction and applications. *Computer Graphics Forum*, 32(6): 1-23. <https://doi.org/10.1111/cgf.12010>
- [9] Davies, R., Twining, C., Taylor, C. (2008). *Statistical Models of Shape: Optimisation and Evaluation*. Springer Science & Business Media. <https://doi.org/10.1007/978-1-84800-138-1>
- [10] Hasler, N., Stoll, C., Sunkel, M., Rosenhahn, B., Seidel, H.P. (2009). A statistical model of human pose and body shape. *Computer Graphics Forum*, 28(2): 337-346. <https://doi.org/10.1111/j.1467-8659.2009.01373.x>
- [11] Alexa, M. (2002). Recent advances in mesh morphing. *Computer Graphics Forum*, 21(2): 173-198. <https://doi.org/10.1111/1467-8659.00575>
- [12] Sumner, R.W., Popovic, J. (2004). Deformation transfer for triangle meshes. *ACM Transactions on Graphics*, 23(3): 399-405. <https://doi.org/10.1145/1015706.1015736>
- [13] Dinh, H.Q., Yezzi, A., Turk, G. (2005). Texture transfer during shape transformation. *ACM Transactions on Graphics*, 24(2): 289-310. <https://doi.org/10.1145/1061347.1061353>
- [14] Elghoul, E., Verroust-Blondet, A. (2013). A segmentation transfer method for articulated models. In *Eurographics 2013, France*, pp. 17-20. <https://doi.org/10.2312/conf/EG2013/short/017-020>
- [15] Xu, K., Li, H., Zhang, H., Cohen-Or, D., Xiong, Y., Cheng, Z.Q. (2010). Style-content separation by anisotropic part scales. *ACM Transactions on Graphics*, 29(6): 0730-0301. <https://doi.org/10.1145/1882261.1866206>
- [16] Bronstein, A.M., Bronstein, M.M., Kimmel, R. (2008). *Numerical Geometry of Non-Rigid Shapes*. Springer Science & Business Media. <https://doi.org/10.1007/978-0-387-73301-2>
- [17] Liu, J., He, X., Huang, X. (2021). An improved registration strategy for aligning incomplete blade measurement data to its model. *Optik*, 243: 167304. <https://doi.org/10.1016/j.ijleo.2021.167304>
- [18] Bronstein, A.M., Bronstein, M.M., Kimmel, R. (2007). Rock, paper, and scissors: Extrinsic vs. intrinsic similarity of non-rigid shapes. In *2007 IEEE 11th International Conference on Computer Vision*, Rio de Janeiro, Brazil, pp. 1-6. <https://doi.org/10.1109/ICCV.2007.4409076>
- [19] Van Kaick, O., Zhang, H., Hamarneh, G., Cohen-Or, D. (2011). A survey on shape correspondence. In *Computer Graphics Forum*. Oxford, UK, pp. 1681-1707. <https://doi.org/10.1111/j.1467-8659.2011.01884.x>
- [20] Botsch, M., Kobbelt, L., Pauly, M., Alliez, P., Lévy, B. (2010). *Polygon Mesh Processing*. CRC Press. <https://doi.org/10.1201/b10688>
- [21] Fischler, M.A., Bolles, R.C. (1981). Random sample consensus: A paradigm for model fitting with applications to image analysis and automated cartography. *Communications of the ACM*, 24(6): 381-395. <https://doi.org/10.1145/358669.358692>
- [22] Liu, R., Zhang, H., Shamir, A., Cohen-Or, D. (2009). A part-aware surface metric for shape analysis. *Computer Graphics Forum*, 28(2): 397-406. <https://doi.org/10.1111/j.1467-8659.2009.01379.x>
- [23] Biasotti, S., Marini, S., Spagnuolo, M., Falcidieno, B. (2006). Sub-part correspondence by structural descriptors of 3D shapes. *Computer-Aided Design*, 38(9): 1002-1019. <https://doi.org/10.1016/j.cad.2006.07.003>
- [24] Hu, R., Wen, C., Van Kaick, O., Chen, L., Lin, D., Cohen-Or, D., Huang, H. (2018). Semantic object reconstruction via casual handheld scanning. *ACM Transactions on Graphics*, 37(6): 1-12. <https://doi.org/10.1145/3272127.3275024>
- [25] Deng, Y., Yao, R.M., Dyke, R.M., Zhang, J. (2022). A survey of non-rigid 3D registration. *Computer Graphics Forum*, 41(2): 559-589. <https://doi.org/10.1111/cgf.14502>
- [26] Sahillioglu, Y. (2020). Recent advances in shape correspondence. *The Visual Computer*, 36(8): 1705-1721. <https://doi.org/10.1007/s00371-019-01760-0>
- [27] Ovsjanikov, M., Ben-Chen, M., Solomon, J., Butscher, A., Guibas, L. (2012). Functional maps: A flexible representation of maps between shapes. *ACM*

- Transactions on Graphics, 31(4): 1-11. <https://doi.org/10.1145/2185520.2185526>
- [28] Ovsjanikov, M., Corman, E., Bronstein, M., Rodolà, E., Ben-Chen, M., Guibas, L., Bronstein, A. (2016). Computing and processing correspondences with functional maps. In SIGGRAPH ASIA 2016 Courses, New York, NY, United States, pp. 1-60. <https://doi.org/10.1145/3084873.3084877>
- [29] Azencot, M., Ben-Chen, M., Chazal, F., Ovsjanikov, M. (2013). An operator approach to tangent vector field processing. *Computer Graphics Forum*, 32(5): 73-82. <https://doi.org/10.1111/cgf.12174>
- [30] Azencot, S., Weißmann, M., Ovsjanikov, M., Wardetzky, M., Ben-Chen, M. (2014). Functional fluids on surfaces. *Computer Graphics Forum*, 33(5): 237-246. <https://doi.org/10.1111/cgf.12449>
- [31] Azencot, E., Corman, M., Ben-Chen, M., Ovsjanikov, M. (2017). Consistent functional cross field design for mesh quadrangulation. *ACM Transactions on Graphics*, 36(4): 1-13. <https://doi.org/10.1145/3072959.3073696>
- [32] Cammarasana, S., Patané, G. (2021). Localised and shape-aware functions for spectral geometry processing and shape analysis: A survey & perspectives. *Computers & Graphics*, 97: 1-18. <https://doi.org/10.1016/j.cag.2021.03.006>
- [33] Rodola, E., Rota Bulò, S., Windheuser, T., Vestner, M., Cremers, D. (2014). Dense non-rigid shape correspondence using random forests. In *Proceedings of the IEEE Conference on Computer Vision and Pattern Recognition*, Columbus, OH, USA, pp. 4177-4184. <https://doi.org/10.1109/CVPR.2014.532>
- [34] Bronstein, M., Bronstein, M.M., Castellani, U., Falcidieno, B., Fusiello, A., Godil, A., Guibas, L.J., Kokkinos, I., Lian, Z., Ovsjanikov, M., Patané, G., Spagnuolo, M., Toldo, R. (2010). Shrec'10 track: Robust shape retrieval. In *Proceedings of the Eurographics Workshop on 3D Object Retrieval (3DOR'10)*, Goslar, Germany, pp. 71-78. <https://doi.org/10.5555/2381147.2381163>
- [35] Dyke, R.M., Stride, C., Lai, Y.K., Rosin, P.L., Aubry, M., Bronstein, A., Bronstein, A., Cremers, D., Fisher, M., Groueix, T., Guo, D., Kim, V.G., Kimmel, R., Löhner, Z., Li, K., Litany, O., Remez, T., Rodolà, E., Russell, B.C., Sahillioglu, Y., Slossberg, R., Tam, G.K.L., Vestner, M., Wu, Z., Yang, J. (2019). Shrec'19: Shape correspondence with isometric and non-isometric deformations. In *Proceedings of the Eurographics Workshop on 3D Object Retrieval (3DOR'19)*, Italy, pp. 1-9. <https://doi.org/10.2312/3dor.20191069>
- [36] Kendall, G. (1977). The diffusion of shape. *Advances in Applied Probability*, 9(3): 428-430. <https://doi.org/10.2307/1426091>
- [37] Requicha, G. (1980). Representations for rigid solids: Theory, methods, and systems. *ACM Computing Surveys*, 12(4): 437-464. <https://doi.org/10.1145/356827.356833>
- [38] Zorin, P., Schröder, T., DeRose, T., Kobbelt, L., Levin, A., Sweldens, W. (2000). Subdivision for modeling and animation. *ACM SIGGRAPH 2000 Course Notes*.
- [39] Jones, M., Baerentzen, J., Sramek, M. (2006). 3D distance fields: A survey of techniques and applications. *IEEE Transactions on Visualization and Computer Graphics*, 12(4): 581-599. <https://doi.org/10.1109/TVCG.2006.56>
- [40] Wenger, R. (2013). *Isosurfaces: Geometry, Topology, And Algorithms*. CRC Press. <https://doi.org/10.1201/b15025>
- [41] Alexa, M., Behr, J., Cohen-Or, D., Fleishman, S., Levin, D., Silva, C.T. (2003). Computing and rendering point set surfaces. *IEEE Transactions on Visualization and Computer Graphics*, 9(1): 3-15. <https://doi.org/10.1109/TVCG.2003.1175093>
- [42] Levoy, M., Whitted, T. (1985). The use of points as a display primitive. Technical report, 85-022, University of North Carolina at Chapel Hill, NC.
- [43] Bronstein, A.M., Bronstein, M.M., Bruckstein, A.M., Kimmel, R. (2009). Partial similarity of objects, or how to compare a centaur to a horse. *International Journal of Computer Vision*, 84: 163-183. <https://doi.org/10.1007/s11263-008-0147-3>
- [44] Pokrass, J., Bronstein, A.M., Bronstein, M.M., Sprechmann, P., Sapiro, G. (2013). Sparse modeling of intrinsic correspondences. *Computer Graphics Forum*, 32: 459-468. <https://doi.org/10.1111/cgf.12066>
- [45] Zhang, H., Sheffer, A., Cohen-Or, D., Zhou, Q., Van Kaick, O., Tagliasacchi, A. (2008). Deformation-driven shape correspondence. *Computer Graphics Forum*, 27(5): 1431-1439. <https://doi.org/10.1111/j.1467-8659.2008.01283.x>
- [46] Lipman, Y., Funkhouser, T. (2009). Möbius voting for surface correspondence. *ACM Transactions on Graphics*, 28(3): 1-12. <https://doi.org/10.1145/1531326.1531378>
- [47] Besl, P., McKay, N.D. (1992). A method for registration of 3-D shapes. *IEEE Transactions on Pattern Analysis and Machine Intelligence*, 14(2): 239-256. <https://doi.org/10.1109/34.121791>
- [48] Memoli, F. (2008). Gromov-hausdorff distances in euclidean spaces. In *Proceedings of the IEEE Conference on Computer Vision and Pattern Recognition Workshops (CVPR)*, Anchorage, AK, USA, pp. 1-8. <https://doi.org/10.1109/CVPRW.2008.4563074>
- [49] Rusinkiewicz, S., Levoy, M. (2001). Efficient variants of the ICP algorithm. In *Proceedings of the Third International Conference on 3-D Digital Imaging and Modeling*, Quebec City, QC, Canada, pp. 145-152. <https://doi.org/10.1109/IM.2001.924423>
- [50] Zhang, J., Yao, Y., Deng, B. (2021). Fast and robust iterative closest point. *IEEE Transactions on Pattern Analysis and Machine Intelligence*, 44(7): 3450-3466. <https://doi.org/10.1109/TPAMI.2021.3054619>
- [51] Kimmel, R., Sethian, J.A. (1998). Computing geodesic paths on manifolds. *Proceedings of the National Academy of Sciences*, 95(15): 8431-8435. <https://doi.org/10.1073/pnas.95.15.8431>
- [52] Crane, K., Weischedel, C., Wardetzky, M. (2013). Geodesics in heat: A new approach to computing distance based on heat flow. *ACM Transactions on Graphics*, 32(5): 1-11. <https://doi.org/10.1145/2516971.2516977>
- [53] Bronstein, A.M., Bronstein, M.M., Kimmel, R. (2009). Topology-invariant similarity of nonrigid shapes. *International Journal of Computer Vision*, 81: 281-301. <https://doi.org/10.1007/s11263-008-0172-2>
- [54] Kim, V.G., Lipman, Y., Funkhouser, T. (2011). Blended intrinsic maps. *ACM Transactions on Graphics*, 30(4): 1-12. <https://doi.org/10.1145/2010324.1964974>
- [55] Chang, W., Zwicker, M. (2008). Automatic registration for articulated shapes. *Computer Graphics Forum*, 27(5):

- 1459-1468. <https://doi.org/10.1111/j.1467-8659.2008.01286.x>
- [56] Saiti, E., Theoharis, T. (2020). An application independent review of multimodal 3D registration methods. *Computers & Graphics*, 91: 153-178. <https://doi.org/10.1016/j.cag.2020.07.012>
- [57] Rustamov, R.M. (2007). Laplace-beltrami eigenfunctions for deformation invariant shape representation. In *SGP '07: Proceedings of the Fifth Eurographics Symposium on Geometry Processing*, Barcelona, Spain, pp. 225-233. <https://doi.org/10.5555/1281991.1282022>
- [58] Sun, J., Ovsjanikov, M., Guibas, L. (2009). A concise and provably informative multi-scale signature based on heat diffusion. *Computer Graphics Forum*, 28(5): 1383-1392. <https://doi.org/10.1111/j.1467-8659.2009.01515.x>
- [59] Bronstein, M.M., Kokkinos, I. (2010). Scale-invariant heat kernel signatures for non-rigid shape recognition. In *IEEE Conference on Computer Vision and Pattern Recognition (CVPR)*, San Francisco, CA, USA, pp. 1704-1711. <https://doi.org/10.1109/CVPR.2010.5539838>
- [60] Aubry, M., Schlickewei, U., Cremers, D. (2011). The wave kernel signature: A quantum mechanical approach to shape analysis. In *IEEE International Conference on Computer Vision Workshops (ICCV Workshops)*, Barcelona, Spain, pp. 1626-1633. <https://doi.org/10.1109/ICCVW.2011.6130444>
- [61] Lipman, Y., Rustamov, R.M., Funkhouser, T.A. (2010). Biharmonic distance. *ACM Transactions on Graphics*, 29(3): 1-11. <https://doi.org/10.1145/1805964.1805971>
- [62] Litman, R., Bronstein, A.M. (2013). Learning spectral descriptors for deformable shape correspondence. *IEEE Transactions on Pattern Analysis and Machine Intelligence*, 36(1): 171-180. <https://doi.org/10.1109/TPAMI.2013.148>
- [63] Corman, É., Ovsjanikov, M., Chambolle, A. (2015). Supervised descriptor learning for non-rigid shape matching. In *Computer Vision - ECCV 2014 Workshops*, Lecture Notes in Computer Science, Zurich, Switzerland, pp. 283-298. https://doi.org/10.1007/978-3-319-16220-1_20
- [64] Donati, N., Sharma, A., Ovsjanikov, M. (2020). Deep geometric functional maps: Robust feature learning for shape correspondence. In *IEEE Conference on Computer Vision and Pattern Recognition (CVPR)*, Seattle, WA, USA, pp. 8589-8598. <https://doi.org/10.1109/CVPR42600.2020.00862>
- [65] Li, X., Iyengar, S. (2014). On computing mapping of 3D objects: A survey. *ACM Computing Surveys*, 47(2): 1-45. <https://doi.org/10.1145/2668020>
- [66] Berg, T.B., Berg, T., Malik, J. (2005). Shape matching and object recognition using low distortion correspondences. In *IEEE Conference on Computer Vision and Pattern Recognition (CVPR)*, San Diego, CA, USA, pp. 26-33. <https://doi.org/10.1109/CVPR.2005.320>
- [67] Zass, R., Shashua, A. (2008). Probabilistic graph and hypergraph matching. In *IEEE Conference on Computer Vision and Pattern Recognition (CVPR)*, Anchorage, AK, USA, pp. 1-8. <https://doi.org/10.1109/CVPR.2008.4587500>
- [68] Zhang, H., Van Kaick, O., Dyer, R. (2010). Spectral mesh processing. *Computer Graphics Forum*, 29(6): 1865-1894. <https://doi.org/10.1111/j.1467-8659.2010.01655.x>
- [69] Masci, J., Rodolà, E., Boscaini, D., Bronstein, M.M., Li, H. (2016). Geometric deep learning. In *SA '16: ACM Siggraph Asia 2016 Course Notes*, Macau, pp. 1-50. <https://doi.org/10.1145/2988458.2988485>
- [70] Xu, K., Kim, V.G., Huang, Q., Mitra, N., Kalogerakis, E. (2016). Data-driven shape analysis and processing. In *SA '16: ACM Siggraph Asia 2016 Course Notes*, Macau, pp. 1-38. <https://doi.org/10.1145/2988458.2988473>
- [71] Halimi, O., Litany, O., Rodola, E., Bronstein, A.M., Kimmel, R. (2019). Unsupervised learning of dense shape correspondence. In *Proceedings of the IEEE/CVF Conference on Computer Vision and Pattern Recognition*, Long Beach, CA, USA, pp. 4370-4379. <https://doi.org/10.1109/CVPR.2019.00450>
- [72] Abdelreheem, A., Eldesokey, A., Ovsjanikov, M., Wonka, P. (2023). Zero-shot 3D shape correspondence. In *ACM SIGGRAPH Asia 2023 Conference Papers*, New York, USA, pp. 1-11. <https://doi.org/10.1145/3610548.3618228>
- [73] Taubin, G. (1995). A signal processing approach to fair surface design. In *Proceedings of the 22nd Annual Conference on Computer Graphics and Interactive Techn (SIGGRAPH '95)*, United States, pp. 351-358. <https://doi.org/10.1145/218380.218473>
- [74] Levy, B. (2006). Laplace-beltrami eigenfunctions towards an algorithm that "understands" geometry. In *IEEE International Conference on Shape Modeling and Applications 2006 (SMI'06)*, Matsushima, Japan, pp. 13-13. <https://doi.org/10.1109/SMI.2006.21>
- [75] Kovnatsky, M.M., Bron, M., Bresson, X., Vandergheynst, P. (2015). Functional correspondence by matrix completion. In *IEEE Conference on Computer Vision and Pattern Recognition (CVPR)*, Boston, MA, USA, pp. 905-914. <https://doi.org/10.1109/CVPR.2015.7298692>
- [76] Nogneng, D., Ovsjanikov, M. (2017). Informative descriptor preservation via commutativity for shape matching. *Computer Graphics Forum*, 36(2): 259-267. <https://doi.org/10.1111/cgf.13124>
- [77] Ren, J., Panine, M., Wonka, P., Ovsjanikov, M. (2019). Structured regularization of functional map computations. *Computer Graphics Forum*, 38(5): 39-53. <https://doi.org/10.1111/cgf.13788>
- [78] Melzi, S., Ren, J., Rodolà, E., Sharma, A., Wonka, P., Ovsjanikov, M. (2019). Zoomout: Spectral upsampling for efficient shape correspondence. *ACM Transaction on Graphics (TOG)*, 38(6): 1-14. <https://doi.org/10.1145/3355089.3356524>
- [79] Rodolà, E., Cosmo, L., Bronstein, M.M., Torsello, A., Cremers, D. (2017). Partial functional correspondence. *Computer Graphics Forum*, 36(1): 222-236. <https://doi.org/10.1111/cgf.12797>
- [80] Ezuz, D., Ben-Chen, M. (2017). Deblurring and denoising of maps between shapes. *Computer Graphics Forum*, 36(5): 165-174. <https://doi.org/10.1111/cgf.13254>
- [81] Ren, J., Melzi, S., Wonka, P., Ovsjanikov, M. (2021). Discrete optimization for shape matching. *Computer Graphics Forum*, 40(5): 81-96. <https://doi.org/10.1111/cgf.14359>
- [82] Vallet, B., Lévy, B. (2008). Spectral geometry processing with manifold harmonics. *Computer Graphics Forum*, 27(2): 251-260.

- <https://doi.org/10.1111/j.1467-8659.2008.01122.x>
- [83] Pinkall, U., Polthier, K. (1993). Computing discrete minimal surfaces and their conjugates. *Experimental Mathematics*, 2(1): 15-36. <https://doi.org/10.1080/10586458.1993.10504266>
- [84] Wardetzky, M., Mathur, S., Kälberer, F., Grinspun, E. (2007). Discrete Laplace operators: No free lunch. *Symposium on Geometry Processing*, 7: 33-37. <https://doi.org/10.2312/SGP/SGP07/033-037>
- [85] Meyer, M., Desbrun, M., Schröder, P., Barr, A.H. (2003). Discrete differential-geometry operators for triangulated 2-manifolds. In *Visualization and mathematics III*, Springer, Berlin, Heidelberg, pp. 35-57. https://doi.org/10.1007/978-3-662-05105-4_2
- [86] Bunge, A., Botsch, M. (2023). A survey on discrete Laplacians for general polygonal meshes. *Computer Graphics Forum*, 42(2): 521-544. <https://doi.org/10.1111/cgf.14777>
- [87] Belkin, M., Sun, J., Wang, Y. (2009). Constructing laplace operator from point clouds in \mathbb{R}^d . In *Proceedings of the Twentieth Annual ACM-SIAM Symposium on Discrete Algorithms, USA*, pp. 1031-1040. <https://doi.org/10.1137/1.9781611973068.112>
- [88] Aflalo, Y., Brezis, H., Kimmel, R. (2015). On the optimality of shape and data representation in the spectral domain. *SIAM Journal on Imaging Sciences*, 8(2): 1141-1160. <https://doi.org/10.1137/140977680>
- [89] Litany, O., Remez, T., Rodola, E., Bronstein, A., Bronstein, M. (2017). Deep functional maps: Structured prediction for dense shape correspondence. In *Proceedings of the IEEE International Conference on Computer Vision, Venice, Italy*, pp. 5659-5667. <https://doi.org/10.1109/ICCV.2017.603>
- [90] Kovnatsky, A., Bronstein, M.M., Bronstein, A.M., Glashoff, K., Kimmel, R. (2013). Coupled quasi-harmonic bases. *Computer Graphics Forum*, 32(2pt4): 439-448. <https://doi.org/10.1111/cgf.12064>
- [91] Neumann, T., Varanasi, K., Theobalt, C., Magnor, M., Wacker, M. (2014). Compressed manifold modes for mesh processing. *Computer Graphics Forum*, 33(5): 35-44. <https://doi.org/10.1111/cgf.12429>
- [92] Boyd, S., Parikh, N., Chu, E., Peleato, B., Eckstein, J. (2011). Distributed optimization and statistical learning via the alternating direction method of multipliers. *Foundations and Trends® in Machine Learning*, 3(1): 1-122. <https://doi.org/10.1561/22000000016>
- [93] Kovnatsky, A., Glashoff, K., Bronstein, M.M. (2016). MADMM: A generic algorithm for non-smooth optimization on manifolds. In *Computer Vision—ECCV 2016: 14th European Conference, Amsterdam, The Netherlands*, pp. 680-696. https://doi.org/10.1007/978-3-319-46454-1_41
- [94] Boumal, N. (2023). *An introduction to optimization on smooth manifolds*. Cambridge University Press. <https://doi.org/10.1017/9781009166164>
- [95] Haas, S., Baskurt, A., Dupont, F., Denis, F. (2017). A framework based on compressed manifold modes for robust local spectral analysis. In *3DOR@ Eurographics, Lyon, France*, pp. 63-66. <https://doi.org/10.2312/3dor.20171054>
- [96] Melzi, S., Rodolà, E., Castellani, U., Bronstein, M.M. (2018). Localized manifold harmonics for spectral shape analysis. *Computer Graphics Forum*, 37(6): 20-34. <https://doi.org/10.1111/cgf.13309>
- [97] Choukroun, Y., Shtern, A., Bronstein, A., Kimmel, R. (2018). Hamiltonian operator for spectral shape analysis. *IEEE Transactions on Visualization and Computer Graphics*, 26(2): 1320-1331. <https://doi.org/10.1109/TVCG.2018.2867513>
- [98] Rampini, A., Tallini, I., Ovsjanikov, M., Bronstein, A. M., Rodolà, E. (2019). Correspondence-free region localization for partial shape similarity via hamiltonian spectrum alignment. In *2019 International Conference on 3D Vision (3DV), Quebec City, QC, Canada*, pp. 37-46. <https://doi.org/10.1109/3DV.2019.00014>
- [99] Postolache, E., Fumero, M., Cosmo, L., Rodola, E. (2020). A parametric analysis of discrete hamiltonian functional maps. *Computer Graphics Forum*, 39(5): 103-118. <https://doi.org/10.1111/cgf.14072>
- [100] Marin, R., Melzi, S., Musoni, P., Bardoni, F., Tarini, M., Castellani, U. (2019). CMH: Coordinates manifold harmonics for functional remeshing. In *3DOR@ Eurographics, Italy*, pp. 63-70. <https://doi.org/10.2312/3dor.20191063>
- [101] Melzi, S., Marin, R., Musoni, P., Bardoni, F., Tarini, M., Castellani, U. (2020). Intrinsic/extrinsic embedding for functional remeshing of 3D shapes. *Computers & Graphics*, 88: 1-12. <https://doi.org/10.1016/j.cag.2020.02.002>
- [102] Azencot, O., Lai, R. (2021). A data-driven approach to functional map construction and bases pursuit. In *Computer Graphics Forum*, 40(5): 97-110. <https://doi.org/10.1111/cgf.14360>
- [103] Marin, R., Rakotosaona, M.J., Melzi, S., Ovsjanikov, M. (2020). Correspondence learning via linearly-invariant embedding. *Advances in Neural Information Processing Systems*, 33: 1608-1620. <https://doi.org/10.5555/3495724.3495860>
- [104] Panine, M., Kirgo, M., Ovsjanikov, M. (2022). Non-isometric shape matching via functional maps on landmark-adapted bases. *Computer Graphics Forum*, 41(6): 394-417. <https://doi.org/10.1111/cgf.14579>
- [105] Hartwig, F., Sassen, J., Azencot, O., Rumpf, M., Ben-Chen, M. (2023). An elastic basis for spectral shape correspondence. In *ACM SIGGRAPH 2023 Conference Proceedings, Los Angeles, CA, USA*, pp. 1-11. <https://doi.org/10.1145/3588432.3591518>
- [106] Liu, H.T.D., Jacobson, A., Crane, K. (2017). A dirac operator for extrinsic shape analysis. *Computer Graphics Forum*, 36(5): 139-149. <https://doi.org/10.1111/cgf.13252>
- [107] Andreux, M., Rodola, E., Aubry, M., Cremers, D. (2015). Anisotropic laplace-beltrami operators for shape analysis. In *Computer Vision-ECCV 2014 Workshops: Zurich, Switzerland*, pp. 299-312. https://doi.org/10.1007/978-3-319-16220-1_21
- [108] Wang, Y., Ben-Chen, M., Polterovich, I., Solomon, J. (2018). Steklov spectral geometry for extrinsic shape analysis. *ACM Transactions on Graphics (TOG)*, 38(1): 1-21. <https://doi.org/10.1145/3152156>
- [109] Melzi, S. (2018). Indicators basis for functional shape analysis. In *Italian Chapter Conference, Italy*, pp. 75-85. <https://doi.org/10.2312/STAG.20181300>
- [110] Corman, E., Solomon, J., Ben-Chen, M., Guibas, L., Ovsjanikov, M. (2017). Functional characterization of intrinsic and extrinsic geometry. *ACM Transactions on Graphics (TOG)*, 36(2): 1-17. <https://doi.org/10.1145/2999535>

[111] Eisenberger, M., Lahner, Z., Cremers, D. (2020).
Smooth shells: Multi-scale shape registration with
functional maps. In Proceedings of the IEEE/CVF

Conference on Computer Vision and Pattern Recognition,
Seattle, WA, USA, pp. 12265-12274.